Reactive ion etching of InP-based quantum cascade lasers

BACHELORARBEIT

zur Erlangung des akademischen Grades
Bachelor of Science
(B. Sc.)
im Fach Physik

eingereicht an der
Mathematisch-Naturwissenschaftlichen Fakultät I
Institut für Physik
Humboldt-Universität zu Berlin

von
Irene La Penna

Betreuung:

1. *Prof. Dr. W. Ted Masselink*
2. *Dr. Mykhaylo Semtsiv*

eingereicht am: *18 April 2019*
Tag der mündlichen Prüfung: 22 Mai 2019

Abstract

Dry etching in a capacitively coupled plasma discharge is applied to InP-based QCLs using an organic-based plasma.
The mechanism of etching for diverse conditions concerning plasma composition, pressure and technical equipment is analyzed and discussed. The requirements for dry etching of InP are defined to be a low pressure regime around 3 μbar and a $CH_4 : H_2 : Ar = 0.5 : 2 : 0.1$ μbar plasma, whereas the specimen has to be fixed to a quartz plate with thermal glue before being placed on the cathode plate to avoid overheating of the sample.
A possible approach for etching of QCL ridges is described, involving a 3-phase processing constituted by dry etching of the InP substrate, wet etching of the Al-containing active region and subsequent dry etching to construct a mesa structure with decent vertical sidewalls and a good degree of selectivity.
The success of such procedure in the fabrication of a laser is still not verified; however, the recipe has been successfully applied to the manufacturing of distributed feedback gratings.

Keywords:
Dry etching, organic based plasma, InP, quantum cascade laser

Abstract

Die vorliegende Arbeit befasst sich mit dem Trockenätzen von aus InP basierten Quantenkasadenlasern in einer kapazitiv gekoppelte Entladung mittels eines organischen Plasmas.
Dass Ätzmechanismus wird in unterschiedlichen Zuständen, die die Zusammensetzung des Plasmas, den Druck und das technische Equipment betreffen, untersucht und diskutiert. Schließlich werden ein niedriges Druckzustand von ungefähr 3 μbar, ein $CH_4 : H_2 : Ar = 0.5 : 2 : 0.1$ μbar Plasma und das Befestigen der Probe auf einer Quartzplatte durch thermisch leitfähigen Klebstoff zu den notwendigen Bedingungen vom Trockenätzen von InP erklärt.
Ein möglicher Ansatz für die Herstellung von QCL-Bauelemente wird als 3-Phasen Prozess beschrieben, wobei der erste Schritt aus dem Trockenätzen des InP-Substrates besteht und der zweite aus dem Nassätzen des Al-enthaltenden laseraktiven Mediums, mit nachfolgendem Trockenätzen. Die so erzeugte Struktur zeigt senkrechte Seitenwände ausreichender Qualität und einen hohen Maß an Selektivität.
Der Erfolg solchem Prozess in der Aufbau von Laser ist nicht bestätigt; das Rezept geling jedoch in die Anfertigung von Gitter mit verteilter Rückkopplung.

Schlagwörter:
Trockenätzen, organisch basiertes Plasma, InP, Quantenkaskadenlaser

A Bianca e Antonio,
Mariella e Federico

Abbreviations

ac	alternate current
BHF/BOE	buffered hydrofluoric acid/buffered oxide etchant
CCP	capacitively coupled plasma
cw	continuous wavelength
dc	direct current
DFB	distributed feedback
MBE	molecular beam epitaxy
MEMS	micro-electro-mechanical-systems
PECVD	plasma-enhanced chemical vapour deposition
QCL	quantum cascade laser
RF	radio frequency
RIE	reactive ion etching
sccm	standard cubic centimeters per minute ($cm^3 \cdot min^{-1}$)
SEM	scanning electron microscope

Contents

1. Introduction

In the early 70s, dry etching was introduced into integrated circuit manufacturing as a revolutionary extension of physical sputtering. It is to no extent an exaggeration to say that since then, this technique has changed human life drastically: to get a sense of this, one should imagine going to work nowadays carrying in the same bag a "portable" computer, a "mobile" phone and a "compact" disc player of three decades ago. Dry etching plays a major role in patterning complex circuits that constitute the core of those common technologies. At a time when semiconductor devices are reaching remarkable sizes in the nanoscale, being able to master the processing technique of dry etching is of essential importance. Most of the research carried out in this field concerned dry etching of silicon- and gallium-based compounds, which are most used in the fabrication of transistors, laser diodes, photodetectors and micro-electro-mechanical-systems (MEMS). The merging of optoelectronics and optical telecommunication encouraged the application of dry etching to In-based alloys, and today the mechanism of dry etching is fully understood and used in the industry. There are still, however, several attempts of optimizing the etching in order to achieve even better results, with the prospect of improving the quality and further reducing the dimensions of those optoelectronic devices.

Dry etching itself is an alternative to wet etching, a method that together with deposition and patterning builds up the fundamentals of microfabrication. Its most favorable characteristic compared to wet etching is the realization of highly anisotropic structures with straight and perpendicular walls, concepts that should be cleared and discussed in the next chapters. The present work focuses on the manufacturing of quantum cascade lasers (QCLs), semiconductor laser devices based on intersubband transitions that emit light in the mid-infrared spectral range. A QCL-wafer consists of a S- or Sn-doped InP substrate where an active region has been grown through molecular beam epitaxy (MBE). The active region is composed by a various number (5 to 200) of alterned InGaAs/InAlAs layers with thicknesses in the range of the nm. The active region is sandwiched between two 300 nm thick InGaAs waveguide layers that have the scope of holding the optical mode centered at the active region. QCLs samples are usually patterned with a 400 nm thick SiO_2 mask and are conventionally processed by wet etching in a $HBr : H_2O_2 : H_2O = 10 : 1 : 50$ solution, that selectively dissolves the InP and the underlying active region without affecting the SiO_2 mask. This method successfully etches laser ridges up to a depth of 10 μm, obtaining the typical isotropical wet etched profile. Extending the technique of dry etching to laser manufacturing would correct several problems encountered in conventionally fabricated QCLs:

- because of its geometry, a wet etched laser has an irregular, crack shaped output beam profile, as shown in figure 1.1(A). In the worst cases, the beam

is split into two at the edge. In order to correct the first aberration, lenses systems are required. This precaution could be avoided using a dry etched laser: for a thin mesa structure, in fact, the ratio between vertical and horizontal length of the active region is closed to unity. The outcoming light, then, would spread equally in both directions when exiting the active region following Huygens-Fresnel principle, resulting in a round beam as visible in figure 1.1(B).

- continuous wavelength (cw) operation heats up the gain medium. Cladding the sides of the laser with In- or Ga-alloys, as well as other dielectrics, allows heat dissipation while electrically insulating the laser structure. The particular form of a dry etched laser should improve these two features.
- confining current into steep and parallel sidewalls should result in a more homogeneous current density inside the laser and reduce leakages.
- dry etching could constitute an alternative way of producing laser facets instead of cleaving. This method would allow curved laser facets to be obtained.
- moreover, dry etching is an essential tool for manufacturing grooves in multisection devices as in submicron gratings.

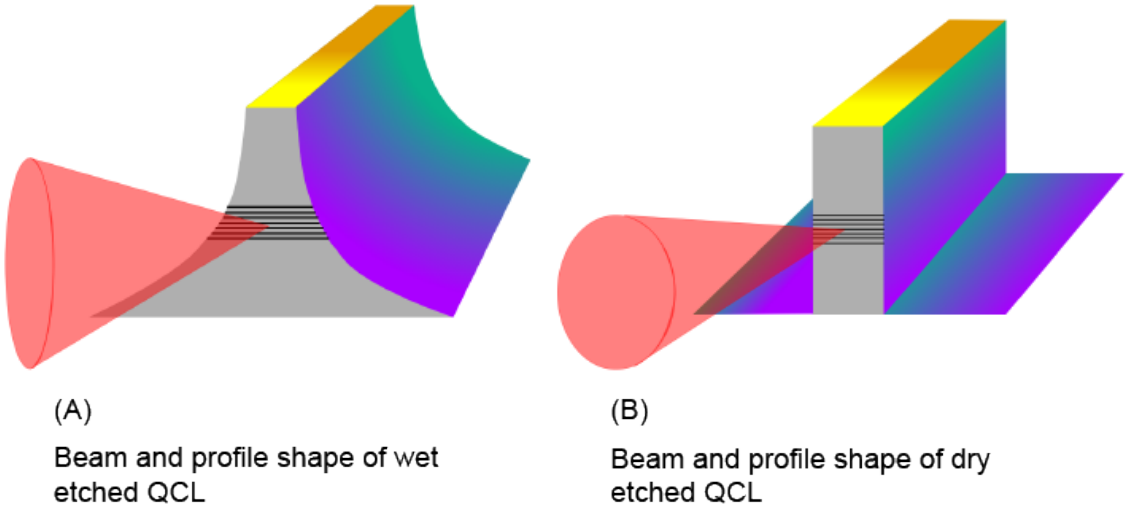

Figure 1.1: wet etched QCL laser ridges have isotropic profiles. Light coming out of the laser is deviated at the aperture of the active region according to Huygens-Fresnel principle, so that a beam exiting from an horizontal fissure will be more expanded in vertical direction. A beam exiting from a square hole, on the other hand, expands equally in vertical and horizontal direction, resulting in a round beam.

Dry etching is performed in a reactor under vacuum by plasma, which is ionized gas. Plasma can be based on diverse chemistries, including bromine- and chlorine-containing gases, but these have the significant disadvantage of being toxic and harmful for both human beings and the instruments. For this main reason, the use of an organic-based plasma is preferred, which is primarily composed by methane and hydrogen. The use of this plasma enables the realization of anisotropic etching with high fidelity to the mask pattern and vertical etched walls, with the advantage

of avoiding the production of toxic gases. On the other hand, the CH_4/H_2 plasma is also responsible for polymer formation on the sample surface and on the walls of the plasma reactor, as should be clarified in the following chapters. As a consequence, the plasma chamber needs to be cleaned from polymer and other residuals after every process, in order to attain reproducibility. Another disadvantageous peculiarity of plasma is its inhomogeneity, which may lead to unpredictable and irregular results even in well-known conditions.

The objective of the project, then, was to find the optimum set of parameters that realizes dry etching of high-aspect-ratio mesas of approximately 10 μm height on QCL wafers, using an organic based plasma.
The main issues to be faced with were reducing the formation of polymer, reaching selectivity, obtaining smooth surfaces and vertical walls, minimizing the etching time and achieving reproducibility.
The parameters that could be varied to attain these goals are the RF power of the generator, the process pressure, the types of gases composing the plasma and the respective fractions in the mixture, and, finally, the process time.
The experiments were successful in deep etching into the InP substrate, but the action of the organic plasma was hindered by the aluminum contained in the active region. A three-phases process consisting of one dry etching, one wet etching and a last dry etching step was developed, which could etch through the active region up to a depth of 13 μm. The wet etch step damages the walls, but the overall aspect of the laser ridge is clear and might be improved by some last cleaning processes to achieve flawless, smooth surfaces and sidewalls.

2. Basics and theory

2.1 Capacitively coupled plasma (CCP)

2.1.1 Setup of a CCP

The CCP used for the experiments essentially consists of two electrode plates placed in a reactor. The gases are let in through side taps that are turned on manually; located on the side is also the opening that brings to the vacuum pump.
A radio-frequency (RF) power supply produces a varying electric field between the two electrodes in the gas chamber, thus generating plasma. How this process takes place will be explained in detail in the next paragraph.
In order to obtain maximum power transfer from the source to the load, the load impedance must match the impedance of the RF generator. This is achieved through an impedance matching network, which transforms the resistive and capacitive characteristics of the plasma. The setup used for the experiments is described in figures 2.1 and 2.2.

2.1.2 Generation of plasma

Let us first analyze the generation of plasma in a discharge operated with direct current. Such a setup is simplified by an electrode plate connected to ground and a parallel one connected to a dc generator, as outlined in figure 2.3 (A). The electric field created between the plates polarizes the gas molecules. If the applied voltage exceeds the value of the striking voltage, the field eventually ionizes the gas atoms, leading to electrical breakdown of the gas. The freed electrons then move towards the anode, while the positive ions are smashed against the cathode. Through the collisions with the quasi-free electrons in the metal plate, the ions can re-gain the missing electrons and become neutral again. However, these collisions can also result in the release of an electron from the cathode, which is then accelerated by the electric field towards the positive electrode. On his way to the anode, the electron can impinge on a gas molecule, thus producing an ion and a free electron. As a consequence, two electrons are now accelerated and a further collision will produce four electrons. The whole process goes on, creating an electrons-ions avalanche in which so many ions as electrons are produced.

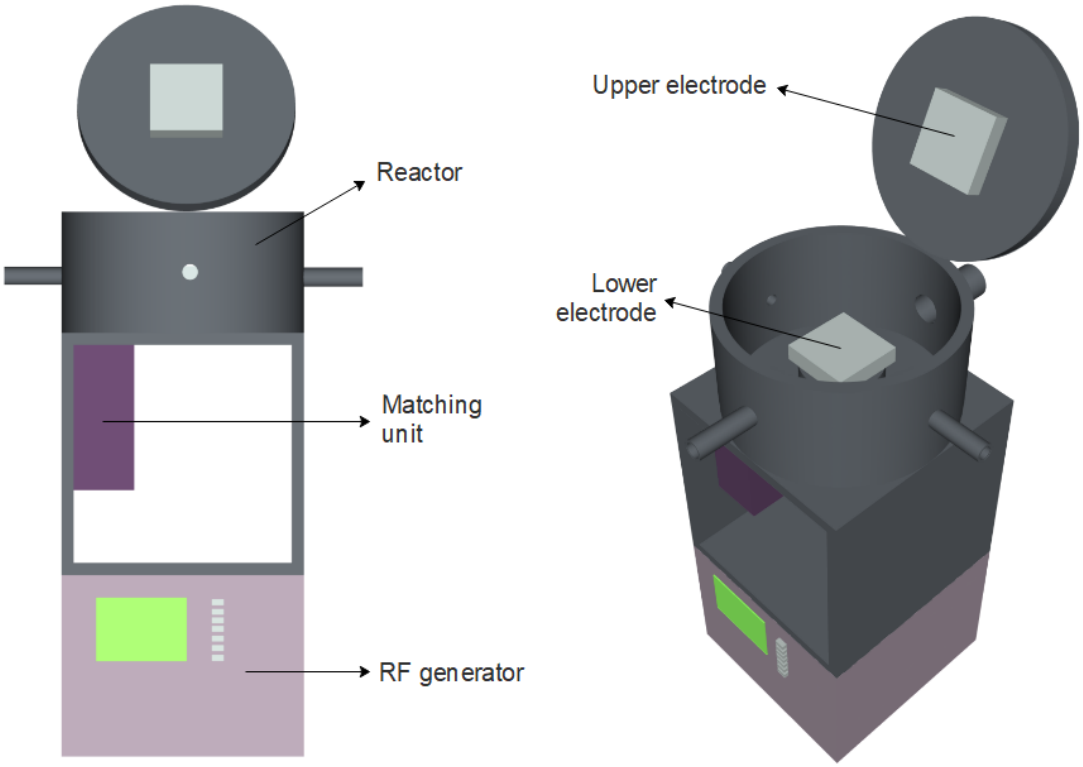

Figure 2.1: instruments and parts composing the experimental setup.

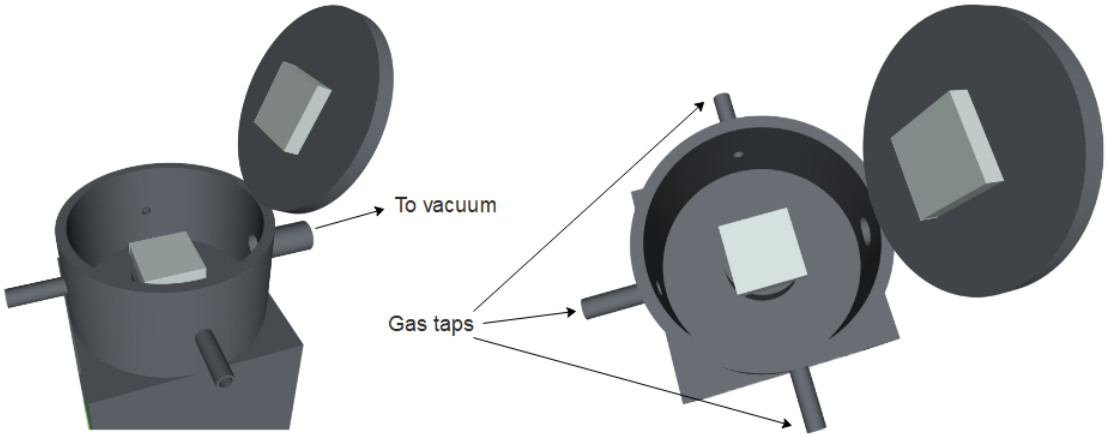

Figure 2.2: interior of the reactor.

2.1.3 Self-bias

The plasma can only sustain itself if an electron current coming from the cathode is allowed, giving rise to the electrons-ions avalanche. If the cathode is covered with a semiconductor or insulator layer or substrate, as it often is the case in the fabrication of nano-devices, this condition is not fulfilled. In the latter situation, in fact, the dielectric layer covering the cathode allows charge accumulation on its surface, but these charges are not mobile as those of a metal and cannot be torn off by the impinging ions.
To solve this problem, an ac power supply to ensure electron current flow in both directions is required. The plasma formation and decay times can vary from 10 ns to

10 μs, so the input frequencies needed for the charged particles not to decay within one half cycle is usually in the radio frequency (RF) range. The most commonly used frequency is 13.56 MHz.
The mechanism for plasma generation in an RF discharge relies on the different mobility of ions and electrons. The equipment, outlined in 2.3 (C), basically consists of two parallel plates, one being grounded and the other powered by the RF supply. The lower electrode plate is isolated from the RF generator by a blocking capacitor, which allows the high frequency current to pass and to generate a varying electric field between the plates. The field ignites a low-density plasma, constituted by an equal number of ions and electrons, as well as neutral molecules. On the powered electrode, the polarity of the voltage changes $13.56 \cdot 10^6$ times every second, and the heavy ions are unable to follow the rapidly varying electric field. The electrons, however, with a mass approximately 100,000 times smaller than the one of the ions, respond immediately to the field and are accelerated towards the powered electrode or away from it every half cycle. This generates a region between the plasma bulk and the chamber walls with a low density of electrons, called the ion sheath.

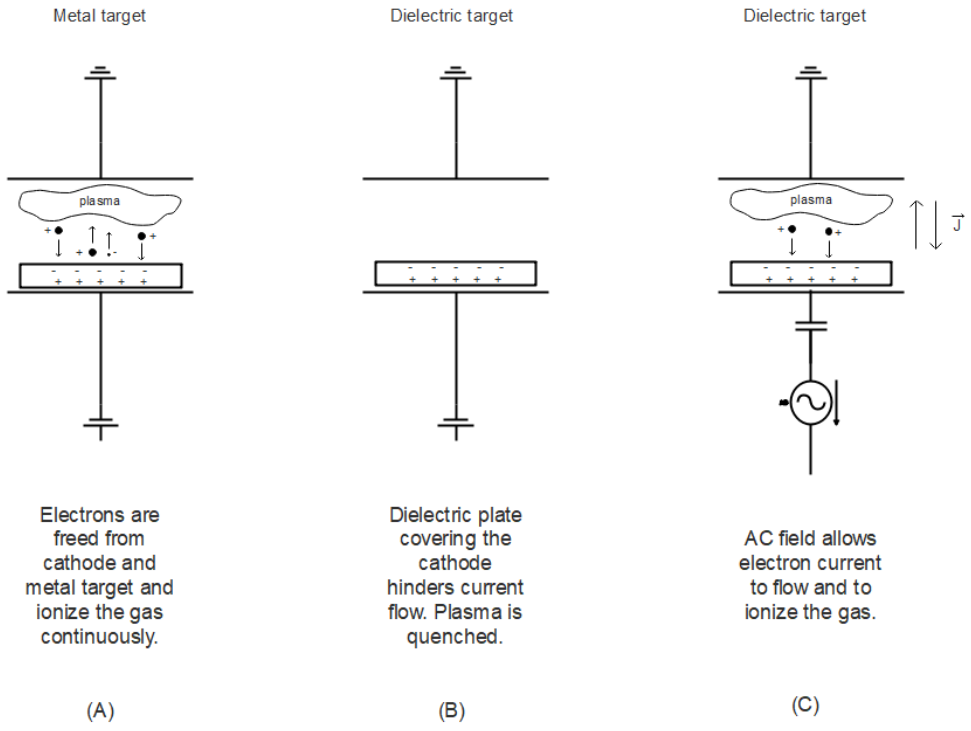

Figure 2.3: schemes of different discharge types.

The electrons impinging on the grounded electrode or on the walls of the reactor are discharged to ground, so those parts of the instrument are always at zero potential. The powered electrode covered with a dielectric plate can be regarded as a perfectly absorbing wall in the theory of plasma [2], meaning that the probability for a low-energy electron to get stuck in it after a collision is closed to unity. The electrons hitting the insulating layer every half cycle accumulate inside the material and are confined there, since the blocking capacitor acts as an impedance to direct current. As a consequence, a negative potential gradually builds up on the powered electrode. In a steady state, the potential looks like (2.4).
The negative dc offset potential is responsible for the etching process and is called

self-bias. It causes ions from the sheath to hit the substrate on the cathode and to actually perform the etching.

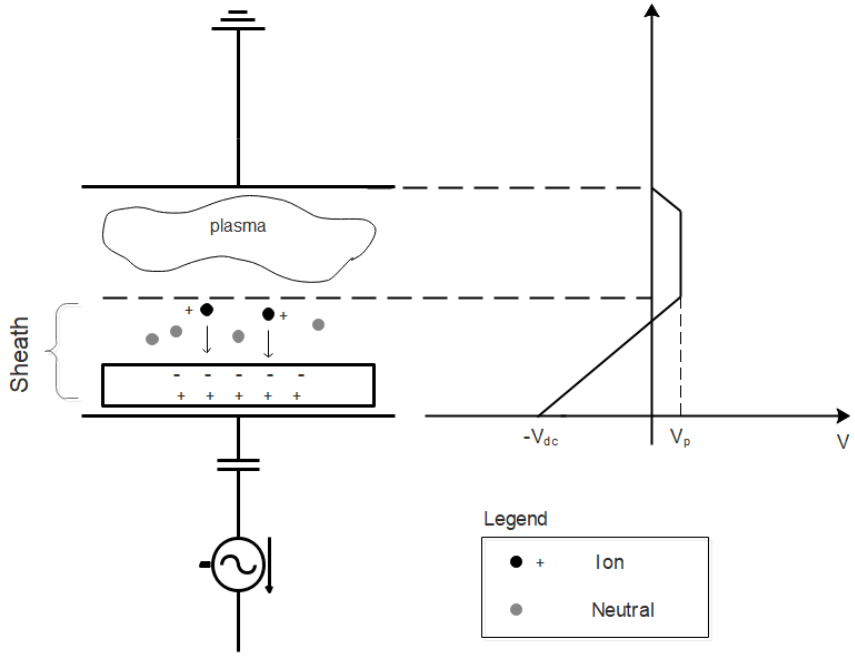

Figure 2.4: potential in the discharge. Plasma has a slight positive charge, while the lower electrode is charged with more electrons every half RF cycle.

2.2 Mechanism of etching and anisotropy

2.2.1 Ion scattering in the sheath

To have a basic understanding of how the etching works, it is useful to examine the motion of ions in the sheath.
As mentioned before, the sheath is the boundary region between plasma and chamber walls or electrodes, characterized by a lack of electrons. The thickness of the sheath is given by the Child-Langmuir equation

$$d_s = \frac{2}{3}\left(\frac{\varepsilon_0}{j_{ion}}\right)^{\frac{1}{2}}\left(\frac{2e}{m_{ion}}\right)^{\frac{1}{4}}(V_p - V_{dc})^{\frac{3}{4}} \tag{2.1}$$

with j_{ion} as the ion current density, ε_0 as the permittivity of vacuum, e as the elementary electric charge, m_{ion} as the ion mass, V_p as the plasma potential and V_{dc} as the dc-bias. This relationship shows that the sheath thickness is small for high-current density plasmas, where the ion density is in the order of 10^{14} cm^{-3}, and the ion current density reaches values of several mA/cm^2. CCPs make use of low-density plasmas, with ion densities between 10^9 and 10^{12} cm^{-3}. With a rough computation, d_s can be estimated to be at least 10 times larger for a low-density plasma than for a high-density plasma.
Another quantity of interest is the mean free path λ, i.e. the average distance that a particle travels from one collision to the next. λ is longer at lower pressures, when less atoms are present in the discharge and the probability of colliding with one of them is smaller.

Ions go through the sheath with almost no scattering for $\lambda \gg d_s$. A CCP, however, generates a low-density plasma; as a consequence, *lambda* is smaller than d_s, and the ions are scattered from the neutrals in the sheath before reaching the wafer. Scattered ions enter the pattern on the sample surface with an angle and hit the uncovered parts from all directions, resulting in irregular and almost isotropic etching. This can be solved by making the pressure inside the reactor lower, so that less atoms exist in the discharge and ion scattering in the sheath is reduced. Ions accelerated towards the wafer gain energy and directionality in the sheath and come almost perpendicular to the substrate surface. In this way, structures with highly anisotropic profiles and high fidelity to mask patterns are produced. A further characteristic of ions travelling highly directionally is the ability to etch fine patterns and wide patterns with the same etch rate, as (2.5) suggests.

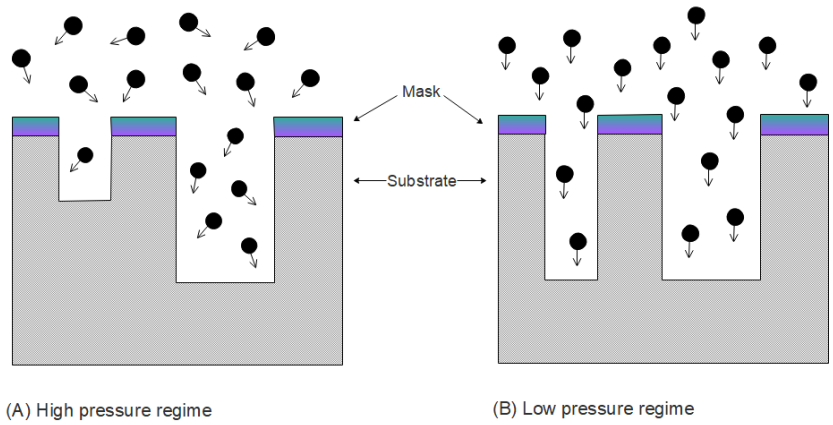

Figure 2.5: ions travelling in diagonal directions do not enter fine and wide patterns with equal probabilities, as perpendicular travelling ions do.

2.2.2 Dry etching process

Plasma is composed of neutral molecules and of other types of particles. When electrons hit neutral molecules, four different reactions can occur:

Excitation: one of the bound electrons of the molecule acquires energy from the colliding electron and is raised to an higher energy state:

$$X + e \rightarrow X^* + e$$

The molecule eventually decays to its ground state through the emission of a photon. This is the cause of the coloured glow of plasma.

Ionization: the electron of the outermost shell gains enough energy to be able to escape the binding forces of the molecule. The molecule acquires a positive charge and is said to be ionized:

$$X + e \rightarrow X^+ + e + e$$

Dissociation: the atoms or groups of atoms building up the molecule can be separated from each other if the energy of the colliding electron is larger than the binding energy of the molecule:

$$XY + e \rightarrow X + Y + e$$

Particles in this state are chemically more reactive than the original molecule would be, and are called radicals. An example of this reaction is the excitation of CF_4 and its following dissociation into radicals $CF_3\cdot$ and $F\cdot$:

$$CF_4 \rightarrow CF_4^* \rightarrow CF_3\cdot + F\cdot$$

Electron attachment: The impinging electron is absorbed by the molecule, turning it into a negative ion:

$$X + e \rightarrow X^-$$

Positively charged ions and radicals are responsible for the etching. Those particles are deflected towards the cathode by the negative bias, and arrive at the wafer surface with relatively high energies (from 100 to 700 eV, depending on the magnitude of V_{dc}). In this way, both chemical etching as well as mechanical etching are possible. In the latter process, the matter composing the sample surface is simply shattered by ion bombardment. On the other side, chemical etching involves reactions taking place between ions and radicals and the molecules of the sample. The products of these reactions are volatile gases that are exhaled in the discharge; as a result, the wafer surface is slowly etched. The etching process for an InP-substrate is illustrated in figure 2.6.

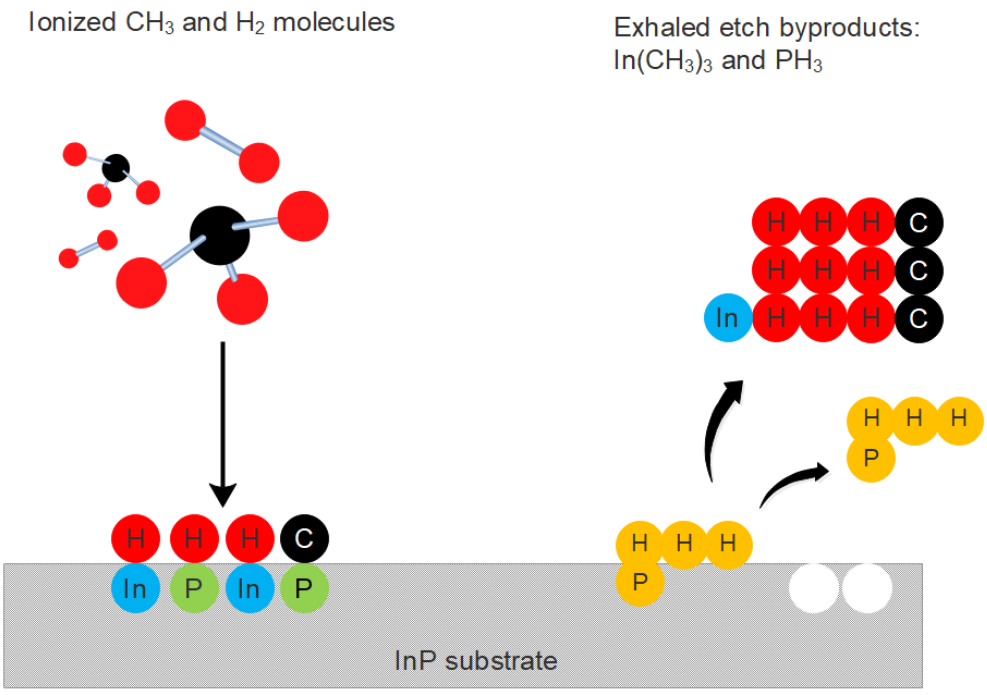

Figure 2.6: scheme illustrating the two main chemical reactions responsible for the etching on an InP substrate. Ionized CH_3 and H_2 molecules reach the surface and react with the material yielding volatile gases that are released in the discharge. Atom per atom, the material is slowly dissolved. Note: the reactions shown in figure are not chemically balanced.

Chemical etching has several advantages with respect to mechanical etching. The most important is selectivity: bombarding a sample with high energy particles that do not chemically react with any element, as noble gases do, sputters away everything at the same speed, independently of the materials composing the surface. If chemical reactions between the atoms on the wafer surface and the impinging ions can occur, however, the reactive atoms are etched away more easily than the unreactive ones and the etching ratio depends on the material composing the surface. This means that every material requires a particular gas recipe in order for chemical etching to take place. The principle of chemical etching actually gives the name to the process of reactive ion etching. A further advantage of chemical etching concerns the quality of the etched surface. Experiments show that etching through particles bombardment leads to rough, perforated surfaces, while etching through reactive ions enables to obtain smooth, clear faces. Last but not least, unreactive particles impinging on the surface with enough energy can be stuck into the material and form bubbles, cracks, and, most importantly, they can damage the crystal structure of the substrate, thus alternating its physical properties.
As mentioned previously, anisotropy is obtained through ions colliding on the sample surface in perpendicular direction. This concept is pictured in figure 2.7. To summarize, then, in order to achieve high fidelity to the mask pattern, good surface morphology and high aspect ratio mesa-structures one should rely on chemical etching by ionized molecules and radicals.

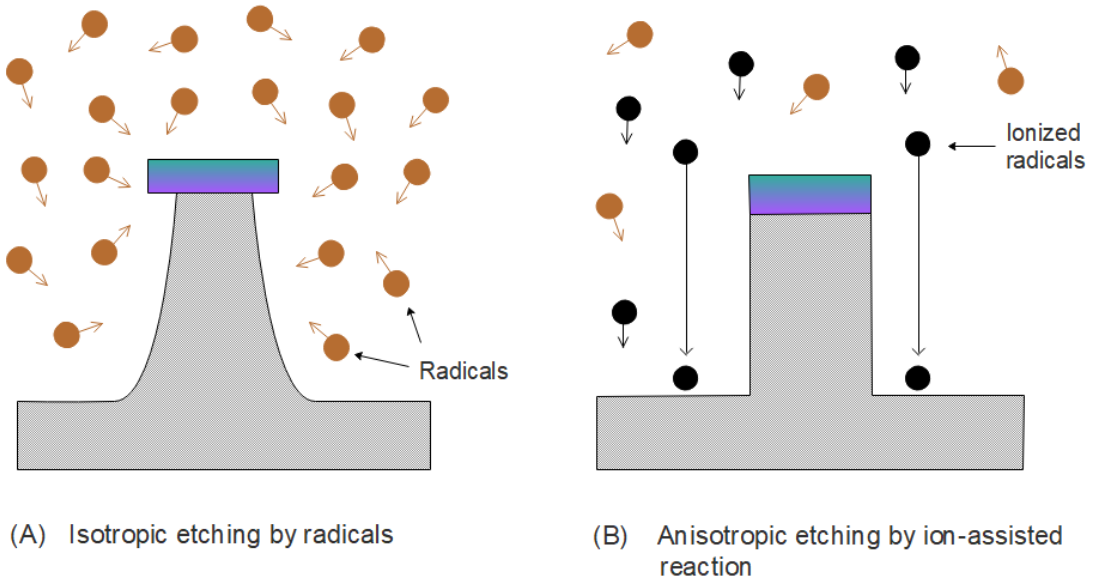

Figure 2.7: anisotropy is realized through the directionality of ions.

2.3 Models and state of research

2.3.1 Organic-based plasma

The first studies of reactive ion etching of InP have been carried out using chlorine-containing gas mixtures, like Cl_2, BCl_3 and CCl_2F_2. Those gases being highly toxic and corrosive constitutes a major issue, which sums up to others concerning the processing of devices. In fact, the etch byproducts from chlorine compounds have

low volatility at temperatures lower than 130°C; moreover, selectivity and structure morphology are reported to be poor, with rough surfaces, strong overcuts and curved sidewall profiles [8, 4]. The study of organic-based plasmas used in RIE has led to positive results with smooth surfaces and perpendicular walls [9], which makes of them the most used in the manufacturing of InP-based devices.
The basic components of the organic-based plasma are methane and hydrogen. They split apart in the discharge into radicals and ions according to following equations [1]:

$$CH_4 \xrightarrow{\text{ionization}} xCH_3 \cdot^* + yCH_2 \cdot^* + zCH \cdot^* + ions$$
$$H_2 \xrightarrow{\text{ionization}} x'H_2^+ + y'H \cdot^* + protons$$

Many reactions occur between these ions and the sample surface, but basically methane radicals are primarily responsible for the depletion of indium, while hydrogen ions preferentially react with phosphorus. Followings are the two main etching reactions taking place on the InP wafer [1]:

$$2P + 3H_2 \rightarrow 2PH_3$$
$$In + 3CH_3 \rightarrow In(CH_3)_3$$

Organic-based plasma is also responsible for other unwanted reactions that result in the formation of carbon-based polymers on the sidewalls. Many are the conditions that promote the growth of polymers; among these are the followings:

- too high pressure inhibiting volatility of etch byproducts, which deposit on the surface.
- high pressure causing accumulation of ions in the mask windows and impeding the etching. If radicals and ions are too many, they react with themselves to form polymers.
- mask charging causes ions to deposit on the mask; if the mask is too thin ions propagate in too large number in the window and are not be able to etch the surface.
- low power and high methane concentrations leading to large numbers of low-energy, low-directional ions and radicals that react with themselves instead of etching the surface and deposit as polymer on the sample structures.

Polymer formation has several undesired effects. It modifies the mesa structure shape and, in the worst cases, prevents from further etching; it deteriorates the surfaces and, ultimately, the polymer film constitutes an unwanted dielectric layer on the whole mesa structure. These polymers are practically insoluble in a variety of organic and inorganic media, but are etchable in an oxygen plasma. A wide range of researches has been made to obstruct and to find the factors that can have an impact on the growth of polymer. One of the most successful [7] involves a cyclical etching process, where etching in a CH_4/H_2 plasma with addition of Ar and O_2 to prevent too large growth of polymer is alternated with cleaning of the sample in an O_2 plasma in order to remove the surplus polymer. Some other studies refer to polymer deposition on the mask as an ally to increase selectivity [10]. In the present work, however, this feature has not been observed.

2.3.2 Features affecting etching

To sum up, many are the factors influencing the etching of InP. Among them, those that could be manipulated with the instruments available for the present project are the RF power, the pressure inside the reactor and the gas fractions in the mixture. It is worth examining the effects that those features are expected to have on the etching, before looking at the experiments:

RF power dependence

Power is directly proportional to the magnitude of the dc self-bias. By this means, changing power automatically has an impact on the degree of ionization of plasma and on the energy and directionality of the ions impinging on the wafer surface. Low powers (approximately 50 W) generate few ions and low dc offsets. This principally results in small etch rates and lack of anisotropy. On the other hand, high powers (approximately 100 W) produce many ions and high dc offsets, leading to faster etch rates and a good level of anisotropy. The existence of many methane ions and reactive atoms in the discharge, however, causes polymer deposition on the sample.

Pressure dependence

In the setup used for these experiment, pressure is varied by changing the amount of gases flowing into the chamber. Higher pressure thus means that more gas molecules are present in the discharge. Radicals and ions produced from methane and hydrogen gather on the surface of the sample and react with themselves to form polymers. Moreover, in a high pressure regime the evaporation temperature of the etch byproducts increases, thus making the otherwise volatile gases stick on the surface as metal-organic polymers. Differently, at low pressures, the substrate is able to adsorb most of the ions and radicals sent to it and deposition of polymers does not take place.

Methane fraction

Methane is an essential gas to perform the etching of InP, as it provides the reactive methyl group which enables the volatilization of indium. In a CH_4/H_2 plasma, the etch rate increases rapidly with methane flow and reaches a maximum at 25%-30% methane flow fraction. After the maximum, the etch rate saturates due to increasing polymer deposition rate, and reproducibility falls short [4].

Argon fraction

Argon has been successfully used in the CH_4/H_2 plasma to increase the etch ratio by mechanical sputtering [8]. This exploits the fact that being a noble gas, argon does not chemically react with any element. Bombarding the substrate with Ar-ions is thus a way of removing polymer from the surface; nevertheless, physical bombardment also has undesired consequences as lack of selectivity, production of rough surfaces and a substantial damage induced below the surface. A further advantage of using argon in the gas mixture is its high power capacity as a plasma constituent.

All those fundamental parameters and their principal effects on the etching process are encapsulated in table 2.1.

factor	**category**	**effects**
pressure	low	high etch rate
	high	- small etch rate - polymer deposition
power	low (50 W)	small etch rate
	high (100 W)	- high etch rate - polymer formation
methane fraction	low (<15%)	small etch rate
	high (>30%)	- saturation of etch rate (polymer formation) - lack of reproducibility
argon addition	advantages	- etching rate increased through mechanical sputtering - high power capacity of plasma
	disadvantages	- rough surface - lack of selectivity - damage induced below the surface

Table 2.1: features affecting etching and their effects at a glance.

3. Experiments

3.1 Instruments and experimental conditions

The experiments were carried out on QCL wafers patterned with a $10 - 20 - 30 - 40 - 50$ μm-stripes SiO_2 mask. The sample preparation is described in appendix A and it is the same for all specimen, if not pointed out in other way.
The experiments were firstly performed on pieces of round wafers placed on the plain aluminum cathode, but during the course of the study the configuration was changed. This should be indicated at the proper moment.
The etching process was initially carried out in a RF driven CCP discharge, backed up by a vacuum rotary pump and a turbomolecular pump; a scheme of the instruments is shown in figures 2.1 and 2.2. In the beginning, the turbomolecular pump was not used and vacuum was achieved by the vacuum rotary pump alone. During the course of the experiments, the apparatus was changed by replacing parts of it. All those changes should be reported in due course.
There are several peculiarities about the plasma chamber that necessarily had to be considered while doing the experiments and while analyzing the data. Those issues arise from the fact that the whole instrumentation is along in years and some of its components are outdated or even damaged. In particular, it is referred to following components:

Pressure gauge

In the beginning, the pressure gauge was situated upon the joint that connected the chamber to the vacuum pump. The gauge was protected from plasma during the etching by a valve that closed the tube where it was placed, and the signal elaborated by the gauge was then sent to a monitor that displayed the pressure magnitude in mbar. Until the old pump was used, the minimal pressure that could be reached inside the chamber was 30 μbar; the new pumping system integrated later was connected to the chamber through a bigger window, in order to achieve a better vacuum. Testing the new pump, it seemed that the vacuum obtained was not better than the previous one; however, measuring pressure with a different pressure gauge and a different monitor revealed that the pressure was actually much lower than before, i.e. less than 0.5 μbar. This raised doubts about the correct working of the pressure gauge until that point, and made all measurements unsure. Given its fragile nature of electronic equipment the pressure gauge is, of course, more than anything else exposed to the risk of being damaged by the plasma. It is possible that this had already happened in the past through plasma going through the valve, ionization of gases adjacent to the gauge, or simply by forgetting the valve open during a process. In addition to this it was also noticed that, after a certain time of using the monitor without turning it off, it would

not show the minimal value of 0.5 μbar. This would change if the monitor was turned off during the etching process. For all these reasons, particular attention was since then paid to the correct usage and functionality of the pressure gauge and of the monitor connected to it. The consequence, however, is that the correct and exact value of the pressure inside the reactor is essentially unknown.

Bias measurement

The bias was measured through the matching unit both directly, by connecting a voltmeter to it, and indirectly by reading its signal output on a computer desktop. During most of the experiments the bias was shown to be positive, which is against the working principles of a CCP used for RIE. This anomaly was explained by testing the bias measurement while varying the RF power, from which resulted that the voltage range supported by the matching unit is from -139 V to +139 V. If the voltage would go below the minimal value, the magnitude would simply not be measured anymore and the sign would flip from negative to positive. For this reason, the correct value of the bias reached by the system during most of the processes is unsure and can only be reported to be below -139 V.

Gas taps

In all laboratories it is convention to measure gas flow in the unit of sccm (standard cubic centimeters per minute, $cm^3 \cdot min^{-1}$), which implies using gas flowmeters to let the gases in and a software to automatically regulate gas flow according to the desired input values. The chamber used for the experiments, however, is not equipped with such instruments, and the gases were let in by simply manually handling the gas taps located on the sides of the reactor, whereas the quantity of gas let in was measured in μbar by computing the difference between the initial pressure inside the chamber and the pressure after the gas was let in. The manual control is, also considering the unreliability of the pressure gauge, an extremely rudimentary way of performing the etching and the measurements; it leads to uncertain values and to problems in trying to test the reproducibility.

Because of those issues, all measurements require to be approximated in order to reach consistency between the different tests.
Further precautions that were carried out include the chamber seasoning and, later on, the cleaning of the quartz plate from etching residuals. Those procedures are described in appendix A and their execution after every etching process was absolutely necessary to ensure the integrity of the instruments and their correct functionality, to avoid sample contamination with etching byproducts deposited on the surfaces and to obtain reproducibility.

3.2 Initial considerations

The large number of parameters to manipulate implied that only one at a time could be varied, in order to acquire reasonable results from the experiments. Based on the results obtained in [7], the process was decided to be made up of a 2 times-repeated cycle of 15 min etching with organic-based plasma alternated with a 5 min oxygen-plasma cleaning. A process would then go like this:

- etching with $CH_4/H_2/Ar$-plasma, 15 min
- cleaning with O_2-plasma, 5 min
- etching with $CH_4/H_2/Ar$-plasma, 15 min
- cleaning with O_2-plasma, 5 min

The inclusion of argon in the mixture and the oxygen cleaning were meant to prevent and reduce polymer formation on the surface.
While the RF power has always been kept constant at 100W, the pressure and the plasma composition have been altered to investigate the etching process. The first recipe to be tried out was a $CH_4 : Ar = 40 : 40\ \mu bar$ plasma with varying H_2 amount. The O_2-plasma was set to 100 μbar for all processes. The pressures inside the chamber, thus, were in the range of $110-130\ \mu bar$, approximately corresponding to $80 - 100\ mTorr$. The second recipe held the methane and hydrogen fractions constant in a $CH_4 : H_2 = 10 : 40\ \mu bar$ plasma and modified the argon fraction in the mixture. After processing, the samples would be cleaved and examined with the scanning electron microscope (SEM); the height of the fabricated structures would then be measured on the images with the help of a software. Some of the images related to the experiments are shown in figure 3.1: they represent the cross-sectional view of the structures etched on the InP-wafer. The active region is recognizable as a stripe between two light-grey lines at a depth of approximately 4 μm in the substrate, while the mask is visible as a light-grey stripe on the top of the structures. What can be immediately noticed from these images is the shining layer covering the etched surface as well as part of the walls. In order to understand what this material was, the sample was shortly wet etched in a solution $HBr : H_2O_2 : H_2O = 10 : 1 : 50$, which is normally used to wet etch the QCL. The intention was to see whether the material would be etched away or not, and to deduce from the result if this layer was not depleted InP or a polymer. As can be seen in figure 3.2, most of the layer was removed by the wet etch dip, meaning that the material contained InP. The fact that parts of it remained on the surface, however, suggested that the material was a metal-organic compound that could not be completely removed by the acid. Another fact in favour of this last hypothesis is the bright, white colour of the layer in the SEM images, meaning that the material is charged, and therefore, that it must be an insulator.

Varying hydrogen flow

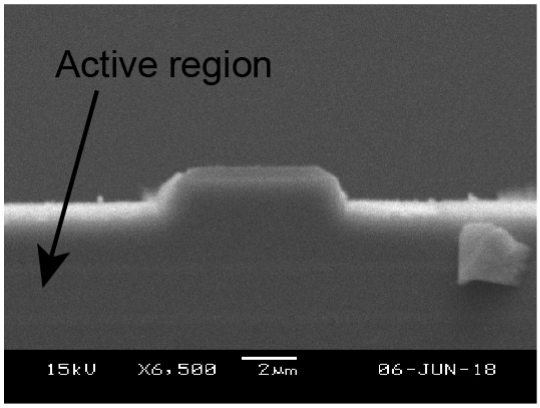

(A) CH_4:H_2:Ar = 40:0:40 µbar

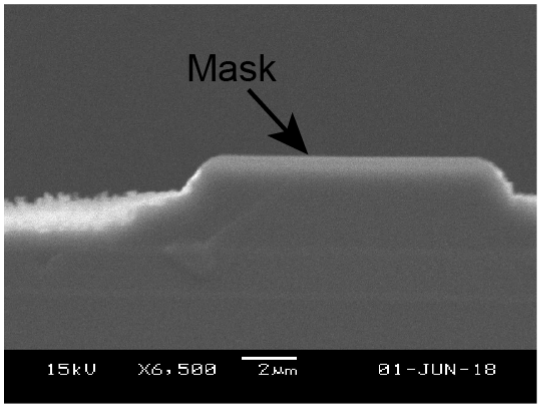

(B) CH_4:H_2:Ar = 40:10:40 µbar

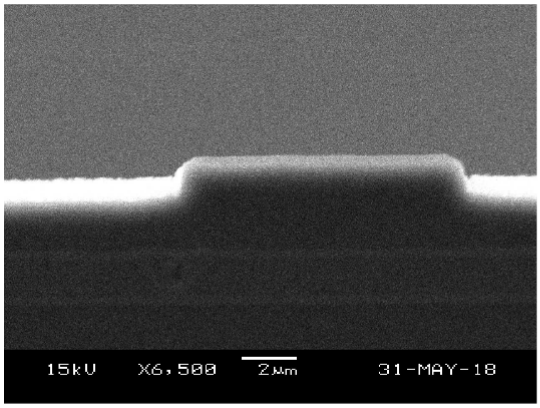

(C) CH_4:H_2:Ar = 40:20:40 µbar

Varying argon flow

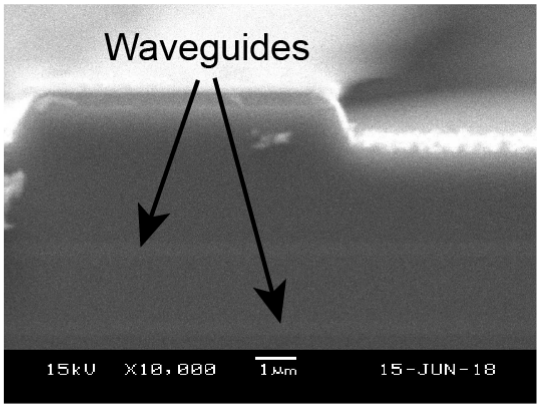

(D) CH_4:H_2:Ar = 10:40:0 µbar

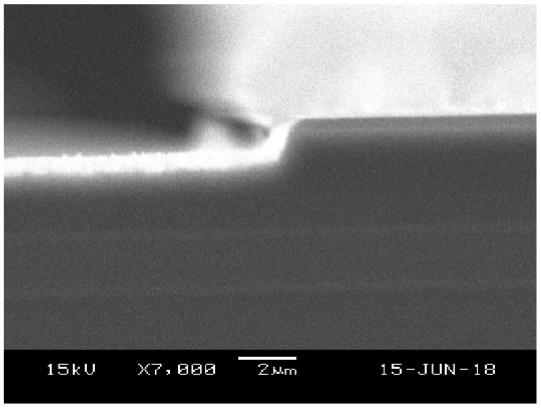

(E) CH_4:H_2:Ar = 10:40:10 µbar

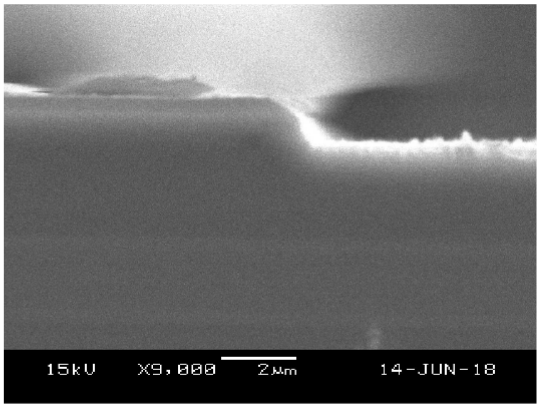

(F) CH_4:H_2:Ar = 10:40:20 µbar

Figure 3.1: cross-sectional view of some structures fabricated in the first experiments. The experimental conditions are reported in the respective caption.

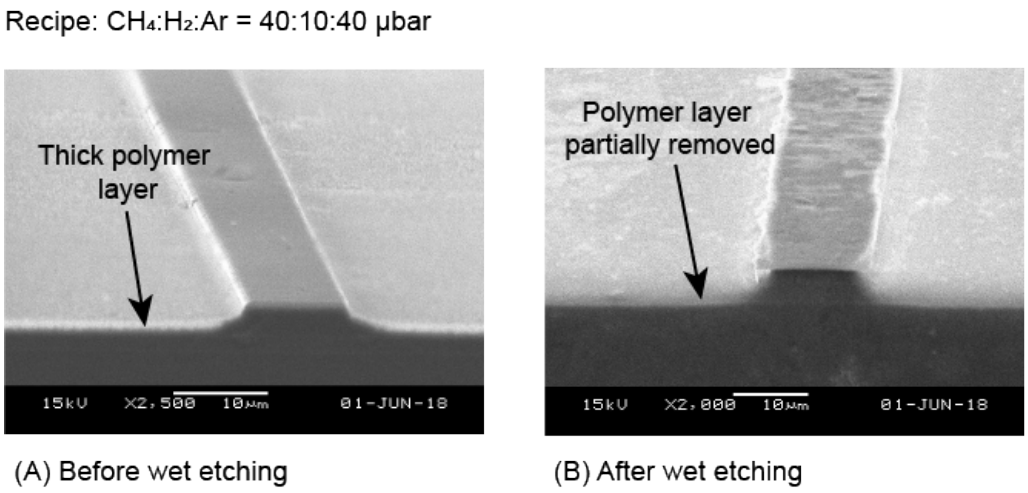

Figure 3.2: a wet etch dip in a $HBr : H_2O_2 : H_2O = 10 : 1 : 50$ solution was performed to study the nature of the residual deposition on the sample surface.

A fundamental aspect that got clear after the first experiments was that the measurements did not play an essential role in this work as the image itself would do. The etched depth, in fact, does not say anything about the quality of the etching since the features that characterize it are others and essentially not quantifiable. Those features, like mesa shape, morphology and profile of the sidewalls, surface roughness and mask integrity are much better explained and analyzed qualitatively through carefully looking at the SEM pictures, and by comparing them to one another the recipe can be optimized until it fulfills the demanded objective. This concept is elucidated by the graphs in figure 3.3, which show both the instability of the process as well as the scarcity of information encapsulated in a graph compared to the power of explanation of one single image.

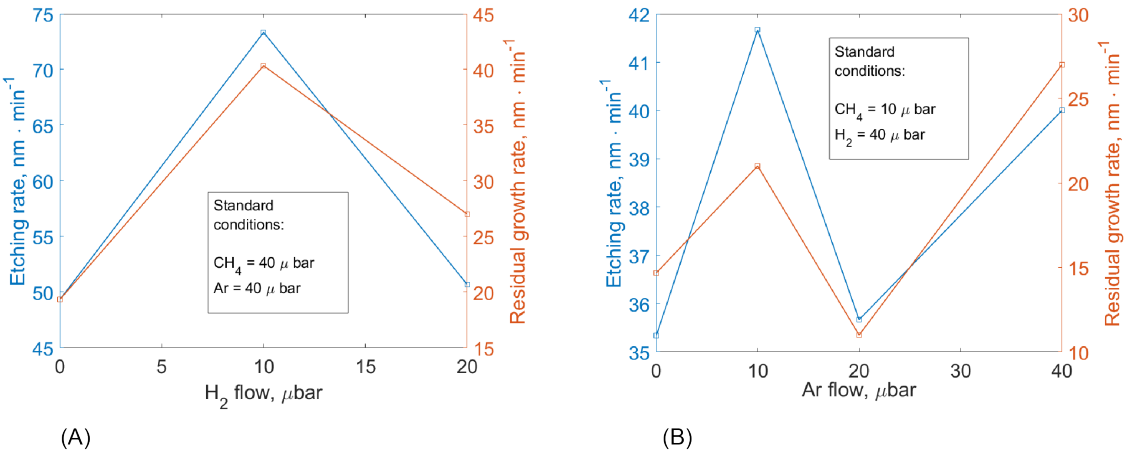

Figure 3.3: etch- and polymer growth rates acquired with the first experiments by varying the H_2 and Ar amounts in the gas mixtures. The data immediately point out the irregularity and instability of the dry etching process.

After those experiments, the first challenges provided by the etching became clear:

- unstable bias
- inhomogeneity of the specimen surface
- binding of organic compounds with the InP on the surface to form non volatile metal-organic polymers
- sloping walls

Those issues were faced one at a time, either by varying the parameters in the recipe or by changing the experimental setting. The section that follows is dedicated to the step-by-step description of those improvements.

3.3 Evolution and progress

3.3.1 Unstable conditions

Many studies implemented in different laboratories mention the use of a quartz plate under the sample during the etching process [9, 4, 8, 6], while in [7] a silicon wafer was used. Following the procedures described in those studies, a quartz plate (thickness 3 mm, diameter 7.62 cm) covering almost the whole area of the electrode was placed under the sample during the etching process. According to the literature, the quartz plate should prevent aluminum from the lower or upper electrode to land on the specimen, thus contaminating it and hindering further etching. The result obtained with this precaution was more stability in the chamber: the bias would stop oscillating and the ingoing RF power would be almost constant over time. This was a first step towards making the etching more reliable and predictable.
The reasons for this outcome have not been further investigated; however, a possible explanation could reside in the working principles of the plasma discharge. As a matter of fact, the value of the bias is determined by the charge accumulated on the lower electrode plate, which depends on the amount of electrons collected on it. The electrons contained in a metal electrode are nearly-free and can be liberated by acquisition of enough energy, for example, through a collision with the ions, or because they perceive the positive plasma potential. The released electrons would then constitute a current between the plates and this movement of charge from the lower electrode unbalances the value of the dc-bias. Electrons stuck in a dielectric electrode, on the other hand, are trapped. Covering the lower electrode with an insulating layer could then have the effect of blocking any leakage current coming from the metal plate, thus stabilizing the dc-bias over time to a value below -139 V. As mentioned in the last section, the value for the bias could not be measured with precision, but by studying its behaviour along with the varying RF power with some practical sense, it can be approximated to -160 V.

3.3.2 Polymer growth

After the unsuccessful outcomes of different gas recipes in the area of polymer removal, it became clear that the deciding factor in order to attain this goal was reducing the pressure. By including the turbo pump in the process, a minimal pressure of 15 μbar inside the reactor was realized. The total process pressure for the etching was thus reduced from approximately 120 μbar to 30 μbar, with remarkably good results in the next experiment shown in figure 3.4.

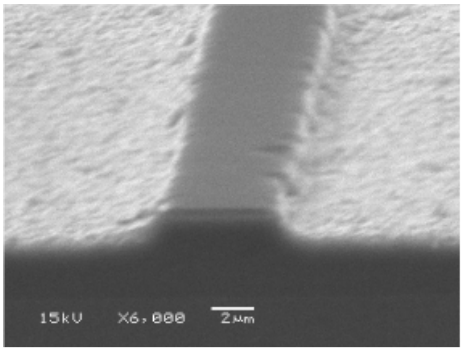

(A) Recipe:
CH_4:H_2:Ar = 40:10:40 µbar, 20 min
O_2 = 40 µbar, 15 min
Cycle repeated 3 times
total pressure during the etching:
120 µbar

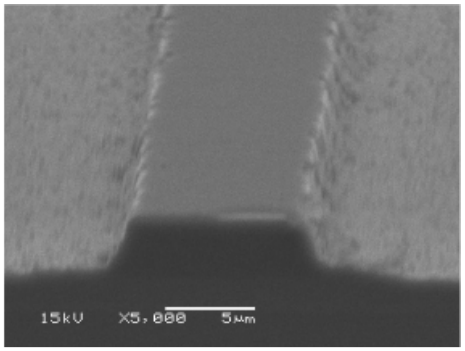

(B) Recipe:
CH_4:H_2:Ar = 3:5:7 µbar, 20 min
O_2 = 10 µbar, 15 min
Cycle repeated 3 times
total pressure during the etching:
30 µbar

Figure 3.4: result obtained by reducing the total process pressure in the discharge. The higher amount of energy and directionality gained by the ions as well as the lack of polymers enhanced the etching.

Another trial at a lower pressure was carried out in order to prove the dependence of residual deposition on the pressure. The outcome, depicted in figure 3.5(A), indicated very explicitly that a lower pressure was necessary to be able to etch deeper without being impeded by the formation of polymer. For this reason, the vacuum pump was replaced with a more powerful one, which was connected to a likewise powerful turbo pump attached to the chamber by a different and bigger hole in its wall. In this occasion, also the pressure gauge was exchanged. With this new setup, an even better vacuum was possible, which enabled reaching a minimal pressure of 0.5 μbar. Setting the total process pressure down from 22 μbar to 3 μbar resulted in a significant success, as can be seen from figure 3.5(B). The sharp edges, the smooth surface and the almost total absence of polymer formations were a clear sign that the etching had to take place at a pressure of about 3 μbar, corresponding to 2.25 $mTorr$. This value is lower than the one found in most of the literature (see [4, 8, 6, 7]); however, the higher pressure reported in those works is compensated, respectively, by higher magnitudes reported for the dc-bias.

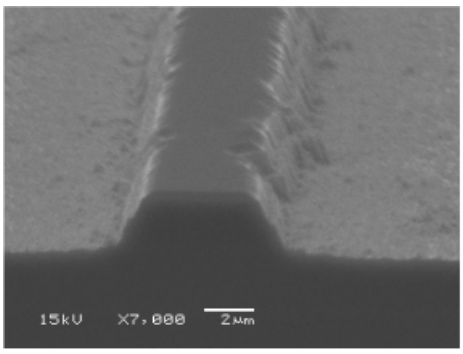

(A) Recipe:
CH_4:H_2:Ar = 1:2:3 μbar, 20 min
O_2 = 3 μbar, 15 min
Cycle repeated 3 times
total pressure during the etching:
22 μbar

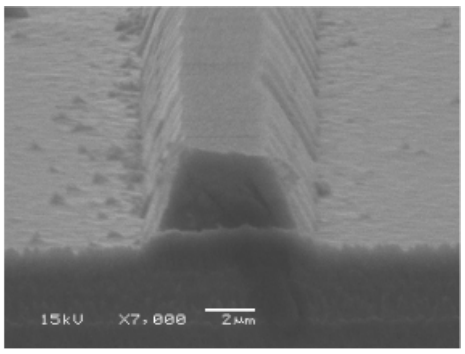

(B) Recipe:
CH_4:H_2:Ar = 0.5:1:1 μbar, 20 min
O_2 = 1 μbar, 15 min
Cycle repeated 3 times
total pressure during the etching:
3 μbar

Figure 3.5: further reduction of the pressure resulted in good-quality surface morphology.

With the tests carried out at a lower pressure, two other issues appeared.

The fact that emerged from the images is the mask erosion occurred during the etching. This is evident in figure 3.6(A) from the incisions on the edges of the mask and from the jagged mesa profile. In figure 3.6(B) the damage inflicted to the mask is less visible, nevertheless, it can be deduced from the small residuals located at the bottom of the sidewall. The SiO_2 mask, in fact, is wet etched and is therefore thicker in the middle and thin on the sides. For this reason, the mask starts being eroded from the sides, and as soon as it is gone the indium phosphide exposed to the plasma gets etched; however, those parts of substrate start being etched later than the windows and in this way the wall assumes the stepped, tilted shape of figure 3.6(B). The sputtering of the mask had not been seen before, therefore, it was associated with the reduction of the pressure, with the idea that the cause resided in the mechanical and chemical sputtering by energetic ions impinging on the surface. Erosion of the SiO_2 mask in an organic plasma for etch depths of 3.5 μm had already been studied and was considered unavoidable in such an environment [5]. It therefore seemed necessary to use other types of mask in order to limit the damage of the InP structures during deep etching.

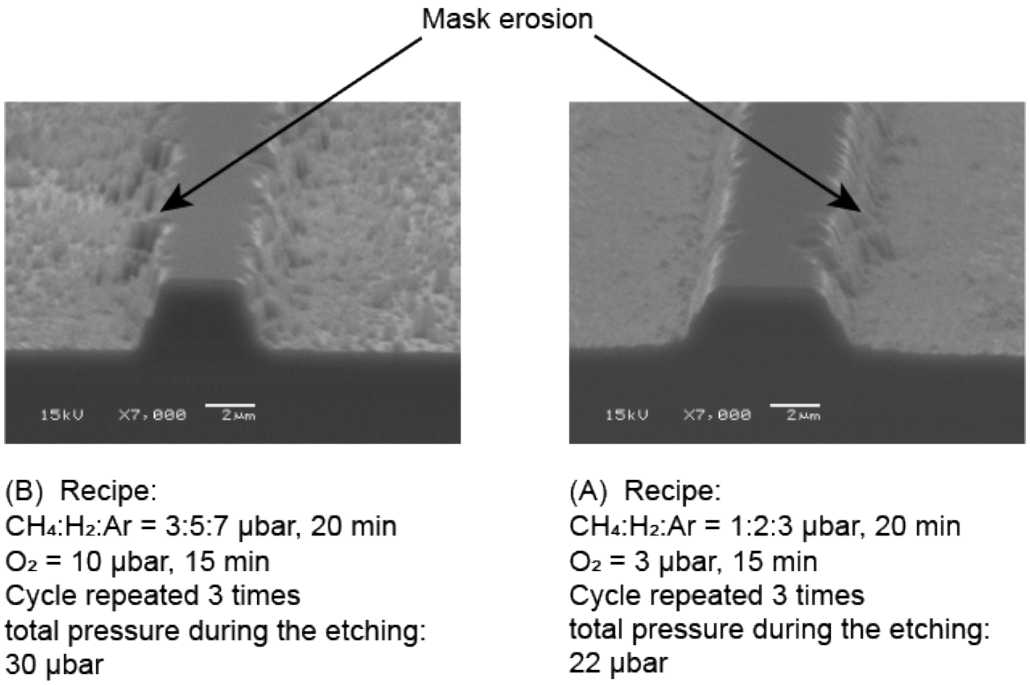

Figure 3.6: residuals on the bottom of the sidewalls suggest that the sides of the SiO_2 mask were sputtered, thus leaving the underlying InP exposed to the plasma.

The second problem shown by specimen etched at low pressures concerned surface homogeneity. A further test was carried out to test the reliability of the recipe that worked so good on the sample depicted in 3.5(B). As can be seen from figure 3.7, it revealed that the etching was not reproducible, meaning that the structures present on the previous sample were only a sort of irregularity on the surface. This made the question of how to make the etching homogeneous over the whole area arise.

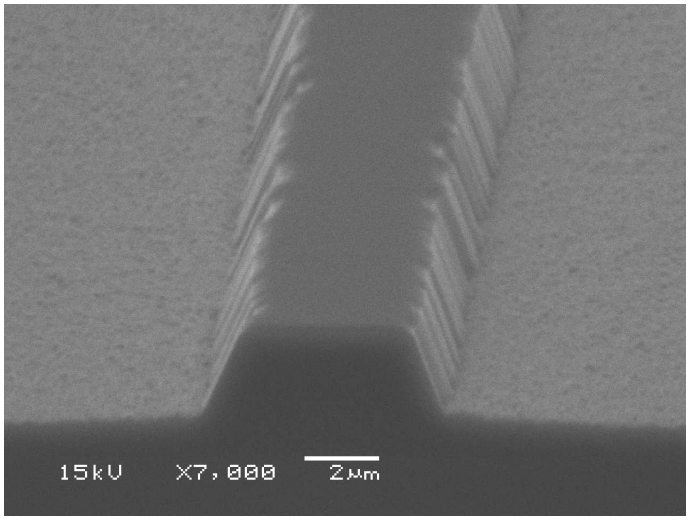

Figure 3.7: sample etched with a $CH_4 : H_2 : Ar = 0.5 : 1 : 1$ μbar plasma for a total process pressure of 3 μbar, 30 min; cleaning with a $O_2 = 1$ μbar plasma, 5 min. The cycle was repeated two times. The shape of this structure demonstrates that the results obtained with last sample using the same etching recipe (see figure 3.5(B)) are not reproducible.

3.3.3 Mask erosion

A deep etching process was performed on a sample for a duration of 3 hours. The process consumed almost the whole mesa structure, depicted in figure 3.8 as a low-height ridge with wavelets on the sides. As can be seen from the image, the active region has been reached, while the mask is not visible on the top. Those facts clearly indicate that the mask had been completely wiped out by the plasma, and that the structure underneath it had already begun to be etched. The need for new types of masks was therefore immediate.

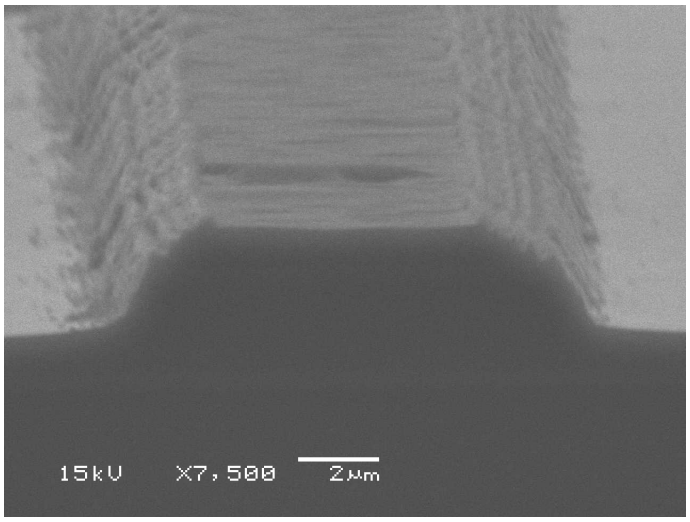

Figure 3.8: sample etched with a $CH_4 : H_2 : Ar = 0.5 : 1 : 1$ μbar plasma, 30 min + $O_2 = 1$ μbar plasma, 5 min. Cycle repeated 6 times for a total duration of 3 hours. While the active region has been reached, the SiO_2 mask has been completely wiped out and the structure has been etched.

The study reported in [3] served as a reference for the patterning of the new masks. The most promising alternatives for obtaining smooth, vertical walls of deep-etched InP-structures were a nickel mask and a double layer $SiO_2 - Ti$ mask. Both were tried out with following results:

Ni-mask

The Ni-layer was deposed with electron beam system and processed by liftoff. For this purpose, a 50 μm stripes mask was used. The Ni-mask was resistant against the effect of plasma, but the etch quality was poor, with extremely rough surface, deposition of polymer on the mask and indented mask profile (see figure 3.9). The latter is a characteristic originating from lift-off patterning, a process that is necessary to prepare this type of mask, since nickel is not etched away by any acid or gas mixture.

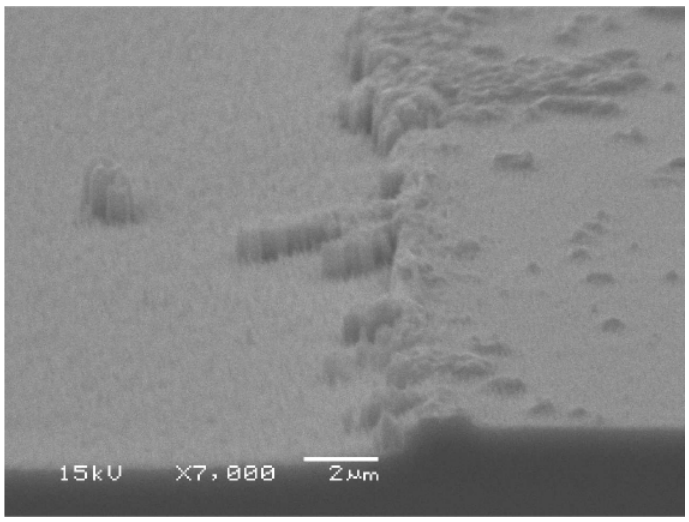

Figure 3.9: sample with Ni-mask etched with a $CH_4 : H_2 : Ar = 3 : 5 : 7$ μbar plasma, 20 min + $O_2 = 10$ μbar plasma, 15 min. Cycle repeated 3 times for a total duration of 1 hour. The mask was resistant to the etching, but its profile had a poor morphology due to the lift-off processing.

Double $SiO_2 - Ti$ mask

A Ti-layer had to be deposed on a SiO_2-layer by PECVD and to be wet etched in a 20% solution of H_2SO_4. The titanium, however, eventually combined with the oxygen in the sputtering discharge and formed a 100 nm thin TiO-film on the substrate. TiO is, on the opposite of pure titanium, extremely resistant to any acid and was not etched even in the most corrosive solutions, like a $HF : HNO_3 : H_2O = 1 : 4 : 5$ solution.

The unsuccessful results obtained with those masks led to an immediate abandonment of the procedures.

A last attempt was performed with a thick gold mask processed by electroplating. The mask was 2.7 μm thick in the middle, and presented two wing-like structures on the sides, which are a typical characteristic of galvanic deposition. The mask is represented from different perspectives in figures 3.10(A), (C) and (E). A 2 hours-etching was implemented with a $CH_4 : H_2 : Ar = 0.3 : 0.6 : 0.6$ μbar plasma, obtaining the structures displayed in figures 3.10(B), (D) and (F). The active region had been reached with the relatively good etch rate of 20 nm/min, and steep sidewalls were obtained. On the other hand, the 2.7 μm gold constituting the central part of the mask had been wiped out in less than 2 hours, and the substrate exposed to the plasma had started being etched.

Before etching

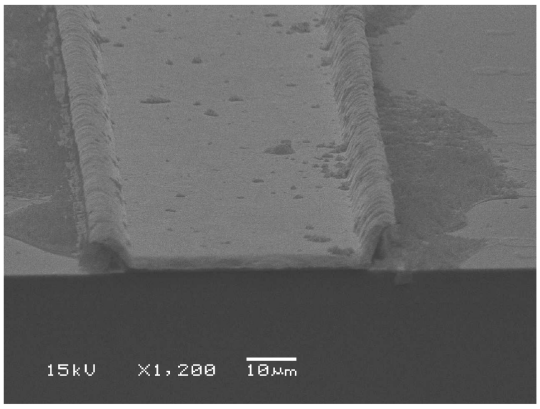

(A)

After etching

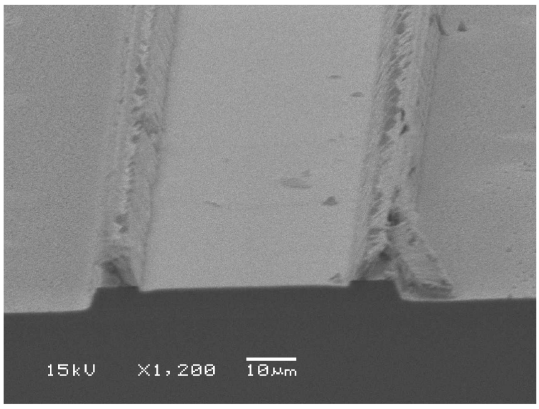

(B)

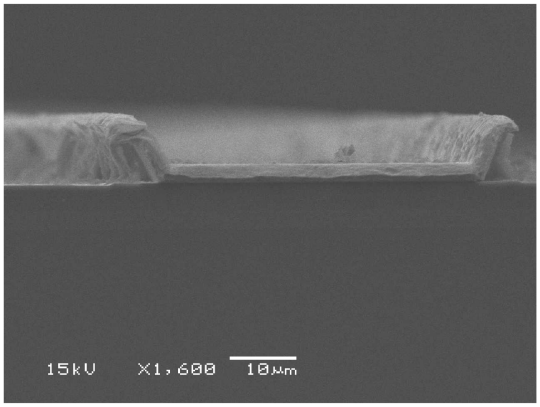

(C)

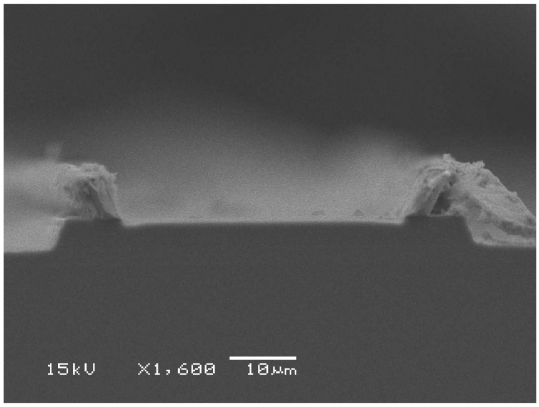

(D)

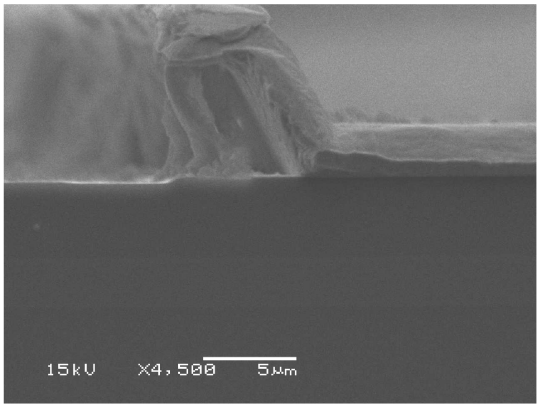

(E)

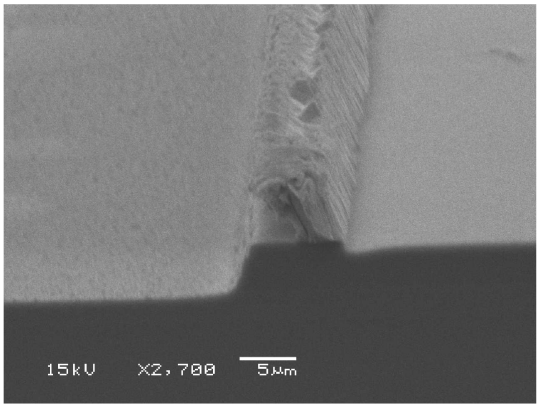

(F)

Figure 3.10: sample with 2.7 μm thick Au-mask. Etching conditions: $CH_4 : H_2 : Ar = 0.3 : 0.6 : 0.6$ μbar plasma, 30 min + $O_2 = 0.5$ μbar plasma, 5 min. Cycle repeated 4 times. The central part of the mask was completely removed and the underlying InP was beginning to be etched.

The fact that the gold mask had been sputtered definitively solved the problem. Gold is in fact a noble metal, i.e. it is inert to plasma. The mask had therefore been removed by mechanical sputtering, which is mostly done by Ar-ions. This meant that the argon fraction in the plasma was too high.

The new strategy to avoid mask sputtering and to be able to etch deeper was thus changing gas mixture. The recipe consisted of 6 cycles of etching followed by an oxygen-plasma cleaning, where the argon fraction was gradually reduced from 14% to 0%, for a total of 3 hours etching. The output, represented in figure 3.11, showed that the etching had dug into the active region generating a good surface morphology. However, the 400 nm thick SiO_2 mask had been reduced to less than 200 nm thickness, and signs of erosion were also visible on the edges. The percentage of argon in the gas mixture had to be kept low over the whole process.

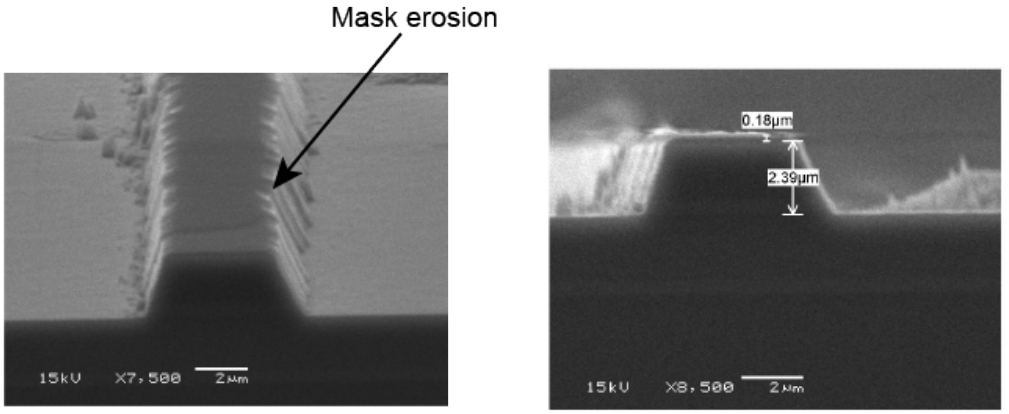

Recipe:

CH_4:H_2:Ar = 0.6:2:0.4 µbar, 30 min + O_2 = 1.5 µbar, 5 min. Cycle repeated 2 times
CH_4:H_2:Ar = 0.6:2:0.2 µbar, 30 min + O_2 = 1.5 µbar, 2 min. Cycle repeated 2 times
CH_4:H_2:Ar = 0.6:2:0.1 µbar, 30 min + O_2 = 1.5 µbar, 2 min
CH_4:H_2:Ar = 0.6:2:0 µbar, 30 min + O_2 = 1.5 µbar, 2 min

Figure 3.11: sample with 400 nm thick SiO_2-mask. The argon fraction was reduced from 40% (in the last recipe) to a maximal value of 14% in the first two cycles, however, mask erosion still occurred.

As a precaution against mask sputtering, the next experiment was performed on a specimen masked with a 800 nm thick SiO_2 mask, realized with 5 hours PECVD. Since deep etching with many cycles of oxygen cleaning is extremely laborious, the process was made shorter by reducing the number of cleaning steps. The idea was that at a lower pressure the polymer is not able to grow in any case, so that exposing the sample to an O_2 plasma would just oxidize the surface and make it more rough, as there is no polymer to remove. The sample was etched for a total time of 6 hours, with approximately 4% argon in the plasma. As can be seen from figure 3.12, the mask was preserved intact, evidenced by the steep, perpendicular walls of the mesa structure; nevertheless, almost no etch occurred.

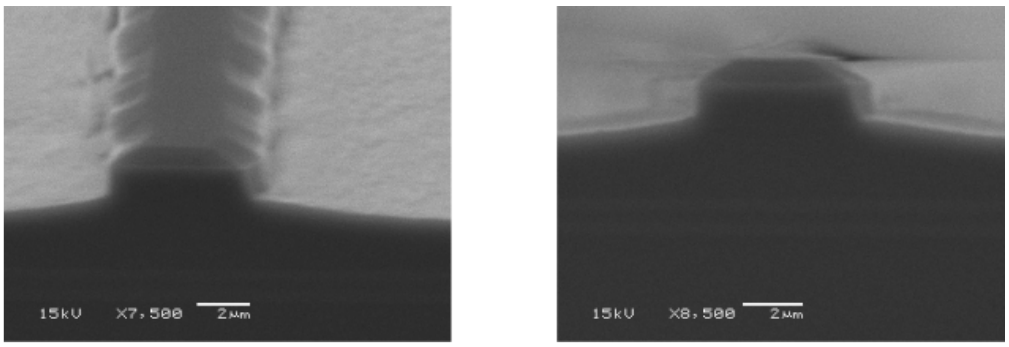

(A) (B)

Recipe:
CH_4:H_2:Ar = 0.6:2:0.1 µbar, 180 min + O_2 = 1.5 µbar, 2 min
CH_4:H_2:Ar = 0.6:2:0 µbar, 180 min + O_2 = 1.5 µbar, 2 min

Figure 3.12: sample with 800 nm thick SiO_2-mask. While mask erosion was prevented, almost no etching occurred.

At this point, a possible explanation was the existence of another uncontrolled parameter affecting the etching, that made the results irregular. The surface of the sample after the etching appeared heterogeneous, as if the etching had taken place along gradient lines. It was noticed, furthermore, that after the etching the quartz plate was hot, and that often the sample would move from the center to the edge of the plate, sometimes it would even fall on the ground of the reactor. The conclusion was that temperature distribution on the surface plays a role in the etching. These facts led to following argument: the quartz plate is thermally conductive, and the sample placed on it is heated by collisions with the plasma. The heat had to be extracted homogeneously from the surface and led into the quartz plate, in order to make the etching pattern regular and to avoid moving of the sample on the plate.

3.3.4 Deep etching and homogeneity

The next challenges, then, were achieving surface homogeneity and deep etching, and the root of both problems were thought to reside in overheating of the sample during the process. The use of water cooled electrodes is reported in [4, 9]. The latter also mentions the use of colloidal graphite to stick the sample to the electrode plate for better thermal contact. The instruments used in this work did not allow cooling of the electrodes, so that the only way to provide thermal extraction was to stick the specimen to the quartz plate with thermal glue. The next experiment was carried out on a plain InP-substrate without cascades, masked with a 800 nm SiO_2 layer, for a total of 6 hours etching, fixed to the quartz plate with thermal paste. The result, displayed in figure 3.13, was quite remarkable: the experiment succeeded in etching at a depth of 11.6 μm and in generating perpendicular walls. The 800 nm thick mask was intact, and the surface was smooth. The nature of the residuals present on the surface and on the mask is unknown.

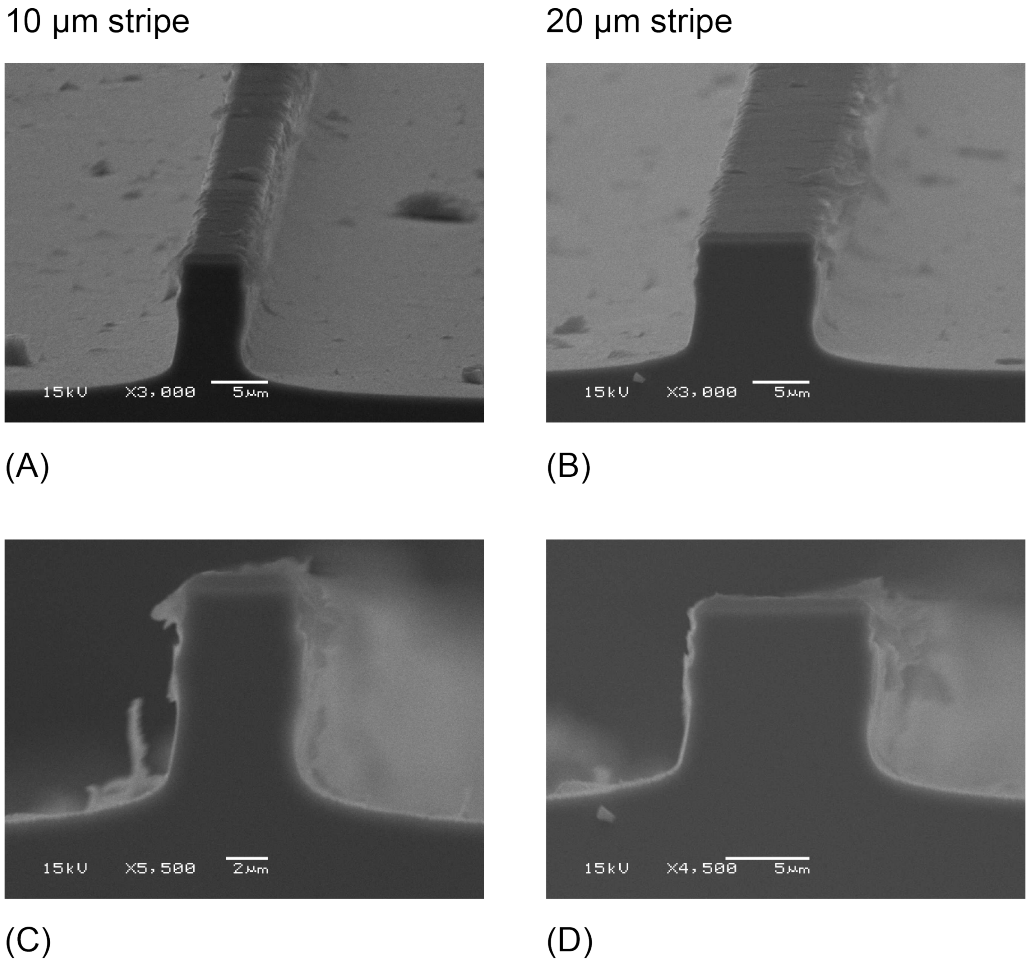

Figure 3.13: plain InP-substrate with 800 nm thick SiO_2-mask. More than 11 μm were etched after 6 hours, and the mask was intact. Smooth surface and perpendicular walls were obtained. Some residuals are present on the surface and on the mask.

The same recipe was tested on another plain InP-sample, fixed to the quartz plate with thermally conductive paste, to prove its reproducibility. This time, the mask was 550 nm thick and the etching process was performed for a total of 8 hours. The same output of the previous experiment was yielded, as shown by figure 3.14, with an etching depth of 11.8 μm.

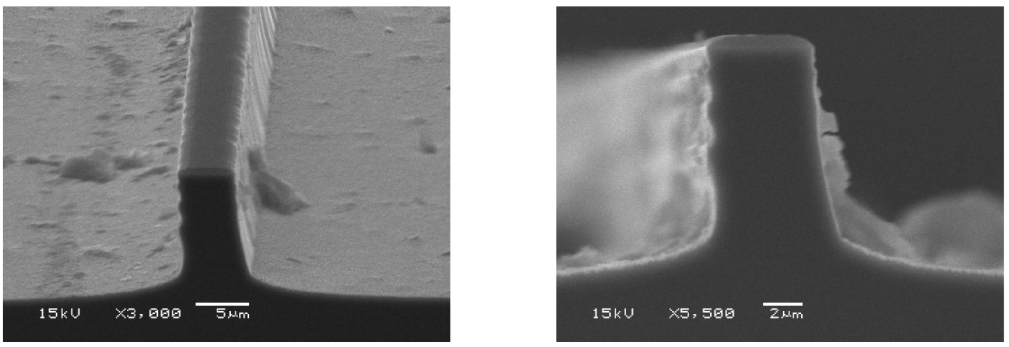

(A) (B)

Recipe:
CH_4:H_2:Ar = 0.5:2:0.1 µbar, 120 min + O_2 = 1.5 µbar, 5 min. Cycle repeated 4 times

Figure 3.14: plain InP-substrate with 550 nm thick SiO_2-mask, etched for 8 hours in the same conditions of 3.13.

The recipe was effective at deep etching plain InP, but its validity had to be proved for QCLs as well. For this purpose, a QCL substrate was patterned with a 600 nm thick SiO_2 mask and etched in the same conditions of the sample in 3.14. In order to make the mesa structure more clean and regular, the mask was dry etched in a 50 μm-stripes pattern according to the procedure described in appendix A. The etching process was shortened by excluding some oxygen cleaning steps, since their aim was almost just conventional at this point. The resulting structures, presented in figure 3.15, have perfectly perpendicular sidewalls; nonetheless, the etching was obstructed at a depth of 4.8 μm, in concurrence with reaching the active region.
According to [4], InGaAs is etchable by an organic-based plasma; moreover, the InGaAs buffer-layer has been removed. For those reasons, it is supposed that the etching has been prevented by the aluminum contained in the InAlAs quantum barriers. The spikes present on the surface might therefore be not depleted aluminum, which creates an impenetrable layer to the plasma.

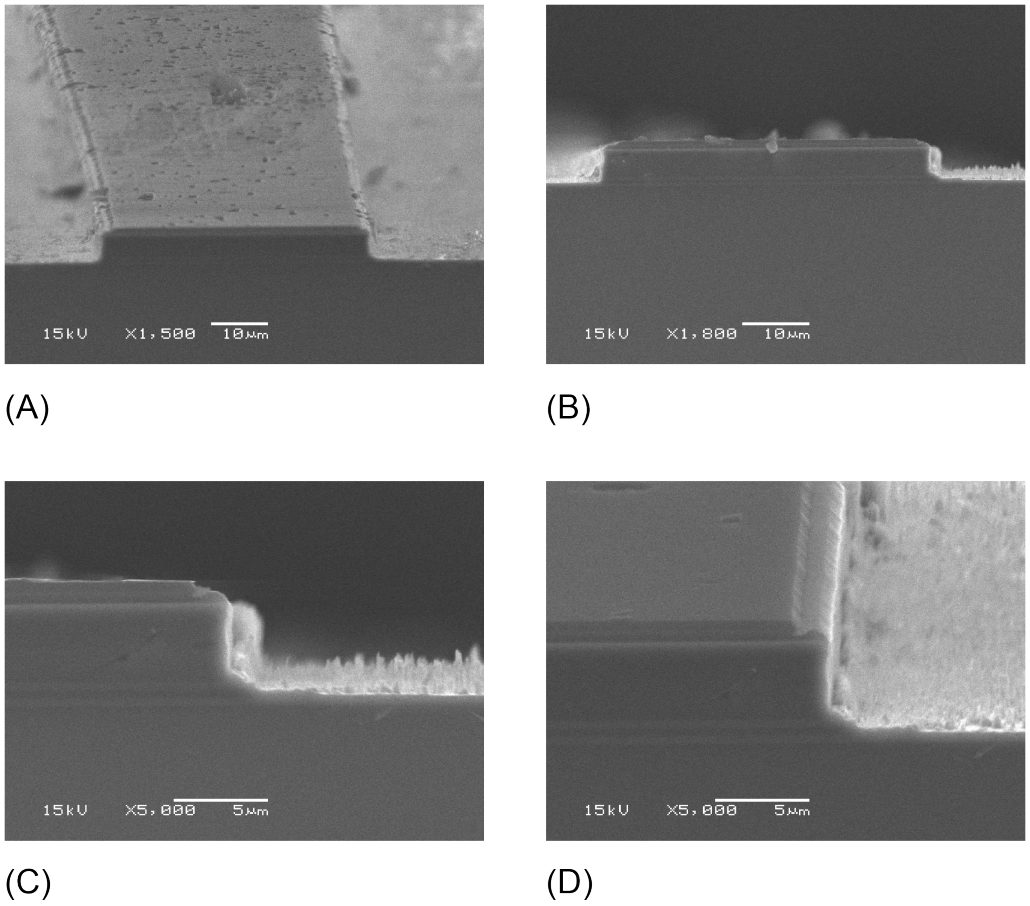

Figure 3.15: Sample with 600 nm thick SiO_2-mask. The layer covering the mask, best visible in (D), is probably a residual of the photoresist used for patterning the mask. The residuals on the surface could be not depleted aluminum.

3.3.5 Etching through the active region

The last challenge in etching QCL structures was going through the active region, in other words, to etch aluminum.
Aluminum is an extremely resistant material and is hardly dry etched (in fact, the gas chamber is made of aluminum), if not with bromine- or chlorine-containing gases. Nevertheless, it can be selectively wet etched in a phosphoric acid (H_3PO_4) solution. The compromise between processing a high-aspect-ratio mesa structure and etching through the cascades, then, was to dry etch the InP substrate in the organic plasma until the active region, then do a quick wet etch dip in a phosphoric acid solution to selectively remove the active region, and to finish and polish the mesa-structure by a last dry etching process. This recipe was used on a sample patterned with a 7.5 μm thick gold mask with the intention of testing the laser right after the process by directly attaching electrical contacts to the mask, but unfortunately, the Au mask was very delicate and the gold stripes were gradually removed during the

etching. Figure 3.16 shows the main stages of the process from different points of view. The wet etching step gravely damages the sidewall, as visible in 3.16(F), but the following dry etching step almost straightens the profile.

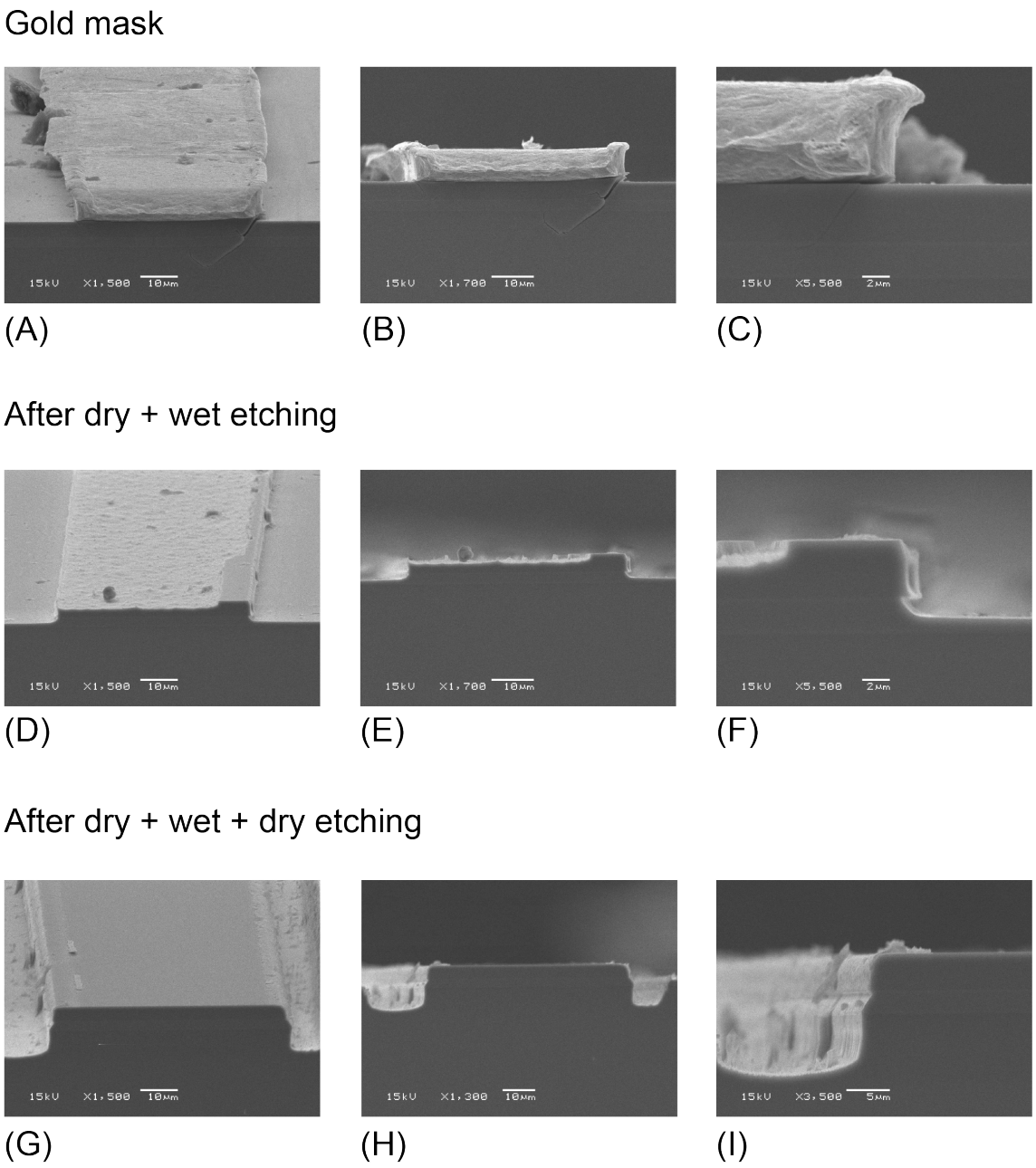

Figure 3.16: A wet etch dip in phosphoric acid was necessary to etch through the active region. The damage induced by the wet etching to the sidewall is almost completely adjusted by the following dry etching step.

4. Conclusion and outlook

4.1 Summary and evaluation

Dry etching of InP-based QCL wafers has been studied under different plasma conditions and by considering the influence of a variety of technical elements. While the RF power was kept constant at 100 W throughout the experiments, most of the investigations concern the total pressure and the gas composition.

The conditions in the gas chamber were first stabilized by placing a quartz plate under the sample, which isolated the wafer from the lower electrode plate creating a homogeneous electric charge distribution on its surface. Different gas mixtures of a $CH_4 : H_2 : Ar$ plasma were tested to find the right composition of plasma, at a pressures of approximately 120 μbar. The problem of polymer growth was initially addressed by cyclically cleaning the specimen with an oxygen plasma; this obstacle, however, was only overcome by reducing the pressure to circa 3 μbar, and later on the O_2 plasma steps were removed from the process. Without polymer, the etching could progress until lower depths, whereas the SiO_2 mask was completely wiped out and the mesa structure underneath eroded by plasma. The attempt of patterning the wafer with different masks was ineffective, but the sputtering of a gold mask during an etching process made clear that the problem of mask erosion resided in the plasma composition: an exceedingly high fraction of argon in the gas mixture performed mechanical etching instead of chemical etching. An updated recipe with a lower percentage of argon ($CH_4 : H_2 : Ar = 0.5 : 2 : 0.1$ μbar) was successfully used to obtain selectivity and perpendicular walls, but the surface of samples appeared extremely irregular. The heat of the quartz plate after the etching and the fact that some specimen would move during the process suggested the involvement of temperature in the etching; the use of thermal glue to extract the heat from the sample solved the problem of inhomogeneity and allowed deep etching to be performed reproducibly on plain InP. The last challenge was represented by the active region: the aluminum contained in the cascades, in fact, prevented from etching a whole QCL mesa structure with plasma. A wet etching step between the two dry etching processes was absolutely necessary to be able to remove the active region, which inevitably defiled the straight, perpendicular walls. The last plasma etching contributed to restore the damage inflicted, but the recipe might be further optimized in such a way that the damage inflicted by wet etching can be completely repaired through etching by plasma.

4.2 Perspectives for future experiments

As mentioned previously, the recipe might be improved in order to correct the step in the sidewall at the height of the active region created by the wet etching phase. This could be performed through a prolonged plasma etching following the wet etching, whereas the latter should be programmed in such a way that the active region layer is totally removed from the surface while minimizing undercutting.
Most importantly, though, the so obtained QCL should be tested and characterized in order to prove its efficiency compared to conventionally fabricated QCLs. First of all the dry-etched QCL mesa structures should be given a quick wet etch dip in hydrobromic acid solution to remove all possible residuals and irregularities and to polish the surface without damaging the structure as a whole. After this precaution, standard procedure can be undertaken to actually construct the laser. The correct functionality of the laser could open the gates to new experiments ranging from fabricating circular or curved laser cavities to processing QCLs with an almost gaussian beam profile. Until now, this technique has been successfully applied to the manufacture of distributed feedback (DFB) lasers.

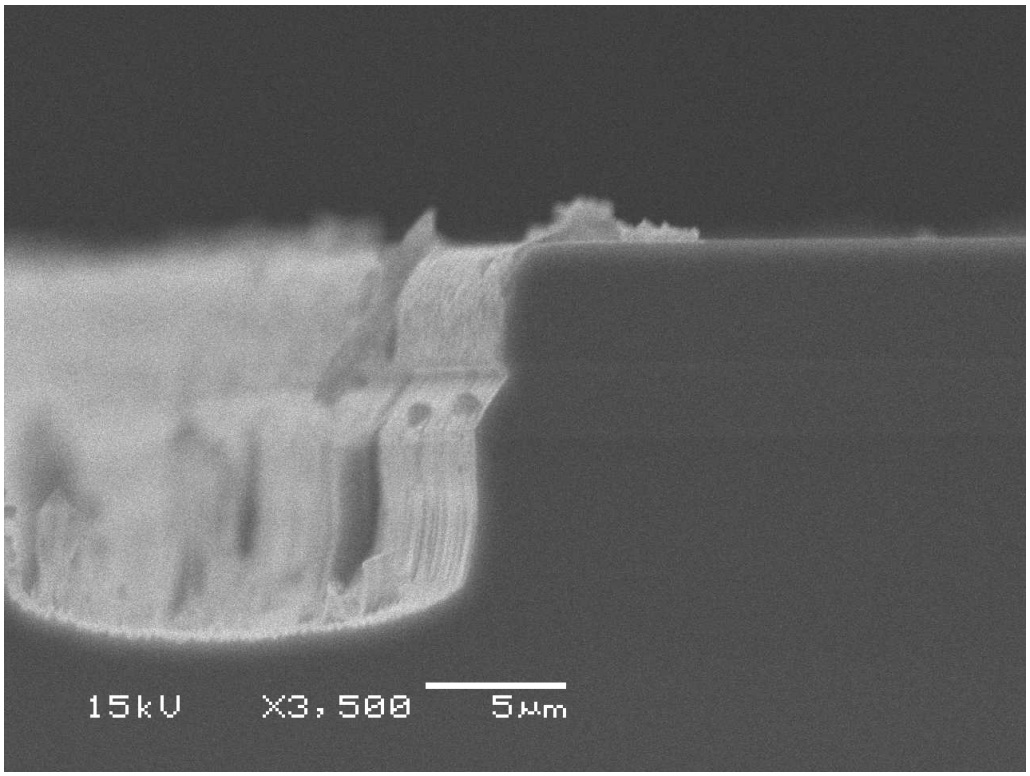

Figure 4.1: profile of QCL after the 3 cycles-etching.

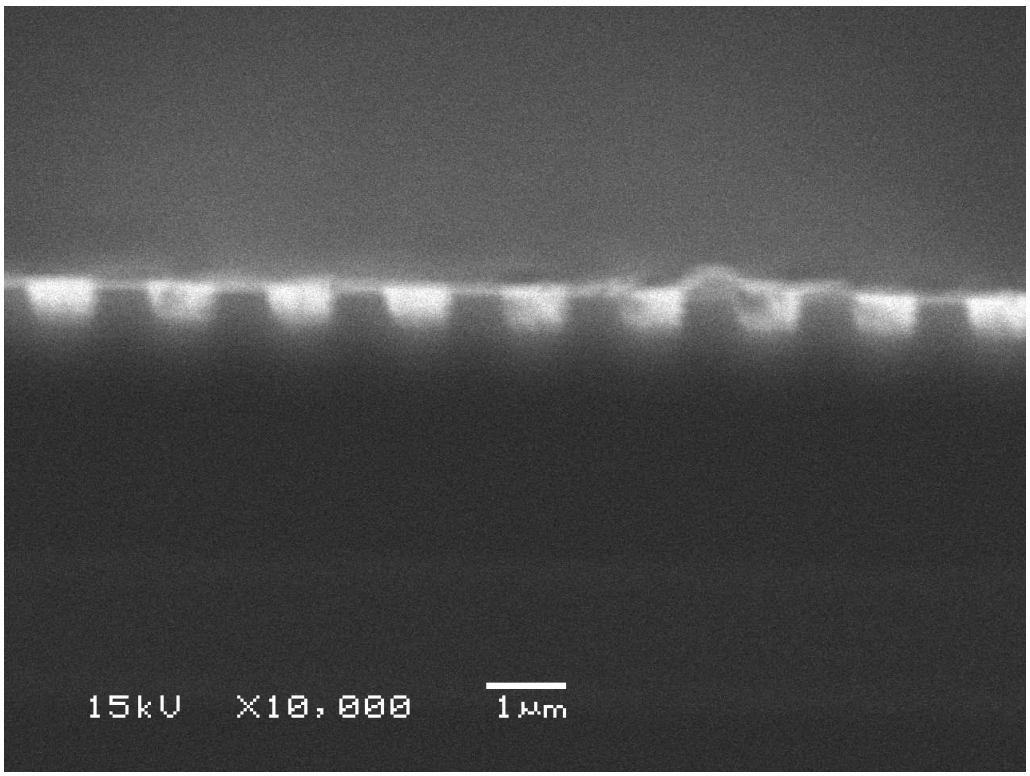

Figure 4.2: cross-sectional view of a DFB grating (courtesy of Alexander Löhr).

A. Experimental procedures

Layers composing the QCL wafer from bottom to top:

- n doped InP (S- or Sn-doping), 350 μm
- InGaAs waveguide, 0.3 μm
- 5-200 InGaAs/InAlAs cascades, $0.2 - 13$ μm
- InGaAs waveguide, 0.3 μm
- n doped InP (S- or Sn-doping), $2 - 3$ μm
- p doped InP, $0.5 - 1$ μm

A.1 Standard sample preparation

SiO_2 layer deposition by plasma-enhanced chemical vapour deposition (PECVD):

- pre-baking in nitrogen at 100°C, 2 minutes
- PECVD with silicon target, $Ar = 36$ $sccm$, $O_2 = 5$ $sccm$. Duration: 3 hours, otherwise 5 hours (where pointed out)
- post-baking in nitrogen at 100°C, 2 minutes

sputtering rate approx. 150 nm/hour
$\Rightarrow result:$ ~ 450 $nm/750$ nm thick SiO_2 film (depending on the sputtering time).

A.1.1 Wet etched SiO_2 mask

Photolithography:

- cleaning of the sample:
  - spray with nitrogen (gas)
  - spin with acetone
  - spin with 2-propanol
  - baking at 150°C, 2 minutes
- attesion promoter: HDMS
- spin coating: 30 s, 3000 RPMs

- baking: 150°C, 2 minutes
- photoresist: AZ5214E (positive)
- spin coating: 30 s, 3000 RPMs
- baking: 115°C, 1 minute
- mask: $10 - 20 - 30 - 40 - 50$ μm stripes
- exposure under UV light: 20 s
- developer: AZ726MIF, 30 s if fresh, otherwise >30 s

SiO_2 Mask patterning:

- wet etching: Buffered hydrofluoric acid (12% HF solution), 1 minute for every 1/2 hour SiO_2 sputtering + 1 minute for safety
- photoresist removal: acetone bath, 2-propanol bath

A.1.2 Dry etched SiO_2 mask

Photolithography:

- cleaning of the sample:
  - spray with nitrogen (gas)
  - spin with acetone
  - spin with 2-propanol
  - baking at 150°C, 2 minutes
- attesion promoter: HDMS
- spin coating: 30 s, 3000 RPMs
- baking: 150°C, 2 minutes
- photoresist: AZ15nXT (negative)
- spin coating: 30 s, 3000 RPMs
- baking: 110°C, 3 minutes
- mask: 450 μm stripes, 50 μm windows
- exposure under UV light: 60 s
- post-baking: 120°C, 1 minute
- developer: AZ726MIF, 5 minutes if not fresh, otherwise <5 minutes

SiO_2 Mask patterning:

- dry etching:
  - only thermal paste
  - RF power: 50 W
  - plasma: $CF_4 = 100\ \mu bar$
  - bias: $\sim$ -60 V
  - time: 25 minutes
- photoresist removal: bath in NI555 at 80°C one night long
- cleaning: acetone bath, 2-propanol bath, dry with N_2 gas

A.2 QCL etching

1^{st} **RIE:**

- quartz plate and thermal paste
- RF power: 100 W
- plasma: $CH_4 : H_2 : Ar = 0.5 : 2 : 0.1\ \mu bar$
- bias: $<$ -139 V
- time: 300 minutes

2^{nd} **selective wet etching of active region:**

$H_3PO_4 : H_2O_2 : H_2O = 10 : 10 : 40$ solution, 60 s (time depends on number of cascades)

3^{rd} **RIE:**

- quartz plate and thermal paste
- RF power: 100 W
- plasma: $CH_4 : H_2 : Ar = 0.5 : 2 : 0.1\ \mu bar$
- bias: $<$ -139 V
- time: 300 minutes

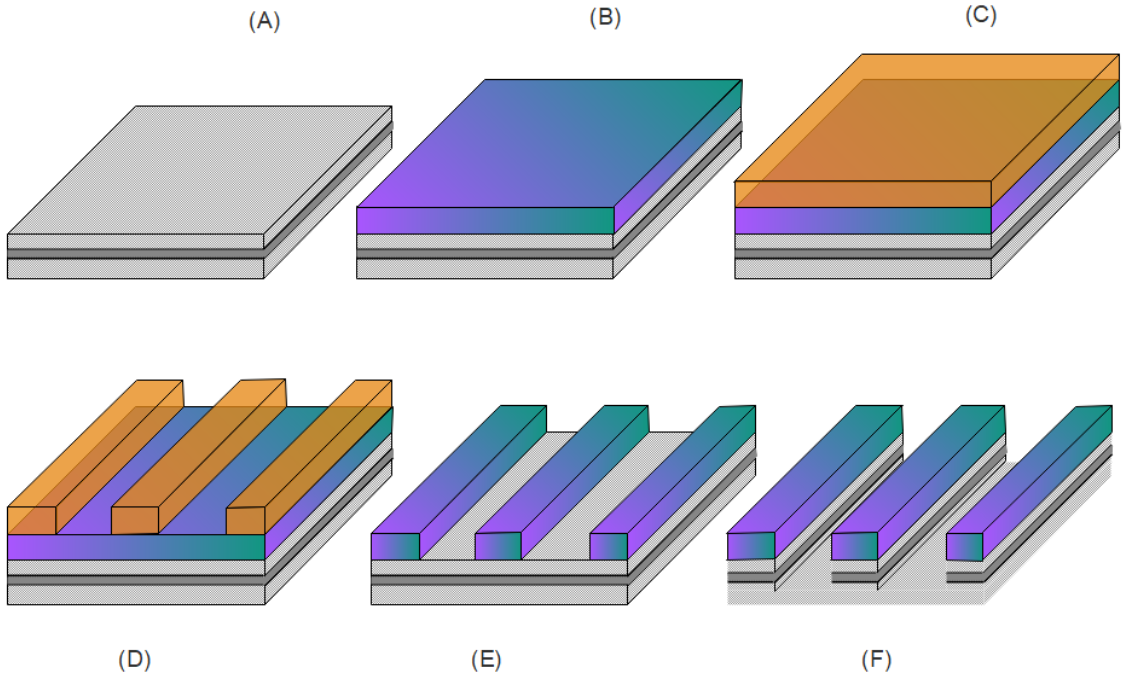

Figure A.1: wafer processing steps: (A) QCL substrate; (B) SiO_2 film; (C) photoresist layer; (D) photoresist mask; (E) SiO_2 mask; (F) QCL after etching

A.3 Chamber and quartz plate cleaning

The reactor and the quartz plate had to be cleaned from polymers and residuals after every process, in order to maintain their functionality and to ensure reproducibility by always processing in the same conditions.

Chamber cleaning

- scratch interior of the reactor, in particular electrode plates, with sand paper, grain size P80
- clean with wipe soaked in acetone, then 2-propanol

Quartz plate cleaning

- scratch surface with sand paper for optical fibers
- clean with wipe soaked in acetone, then 2-propanol

Bibliography

[1] Beck, Patricia ; Derickson, Dennis ; Kellert, Forrest ; Bagwell, Tim: Effects of Hydrogen on InP Light-Emitting Devices Etches in a Methane-Hydrogen Environment. In: *Seventh International Conference on Indium Phosphide and Related Materials*, IEEE, 1995

[2] Bronold, F. X. ; Fehske, H.: Absorption of an Electron by a Dielectric Wall. In: *Physical Review Letters* 115 (2015), nov, Nr. 22

[3] Grover, Rohit ; Hryniewicz, John V. ; King, Oliver S. ; Van, Vien: Process development of methane-hydrogen-argon-based deep dry etching of InP for high-aspect-ratio structures with vertical facet-quality sidewalls. In: *Journal of Vacuum Science and Technology B* 19 (2001), sep

[4] Hayes, T. R. ; Dreisbach, M. A. ; Thomas, P. M. ; Dautremont-Smith, W. C. ; A., Heimbrook L.: Reactive ion etching using CH_4/H_2 mixtures: Mechanisms of etching and anisotropy. In: *Journal of Vacuum Science and Technology B* 7 (1989), Sep/Oct

[5] Lee, B. T. ; Hayes, T. R. ; Thomas, P. M. ; Pawelek, R. ; Sciortino Jr., P. F.: SiO_2 mask erosion and sidewall composition during CH_4/H_2 reactive ion etching of $InGaAsP/InP$. In: *Applied Physics Letters* 63 (1993), dec

[6] McNabb, J. W. ; Temkin, H. G. ; Logan, R. A.: Anisotropic reactive ion etching of InP in methane/hydrogen based plasmas. In: *Journal of Vacuum Science and Technology B* 109 (1991), nov

[7] Schramm, Jeff E. ; Babic', Dubravko I. ; Hu, Evelyn L. ; Bowers, John E. ; Merz, James L.: Fabrication of high-aspect-ratio InP-based vertical-cavity laser mirrors using $CH_4/H_2/O_2/Ar$ reactive ion etching. In: *Journal of Vacuum Science and Technology B* 15 (1997), Sep/Oct

[8] Su Yu, Jae ; Tak Lee, Yong: Parametric reactive ion etching of InP using Cl_2 and CH_4 gases: effects of H_2 and Ar addition. In: *Semiconductor Science and Technology* 17 (2002), feb

[9] Van Gurp, G. J. ; Jacobs, J. M.: Dry etching of InP, applied to laser devices. In: *Philips Journal of Research* 44 (1989), Nr. 1, S. 211–239

[10] Yamamoto, Norio: Dependence of selectivity on plasma conditions in selective etching in submicrometer pitch grating on InP surface by CH_4/H_2 reactive ion etching. In: *Journal of Applied Physics* 9 (2011), apr

Acknowledgements

I take this chance to express my gratitude to Prof. W. T. Masselink for having provided me with this great opportunity and with the necessary equipment, not to mention a very stimulating working environment.

I would like to thank all of those who in some way supported me during this experience:

all the colleagues of the FET team, in particular:
Yohei Matsuoka
Christian Golz
Karin Braune
Iris Newton
Alexander Löhr
Jan Kischkat
David Alcer
Jan Tòmko
Elfi Renger
Paolo La Penna
Giovanni La Penna
Paolo Politi
Amine El Ouadrassi
my ex bicycle and by new loyal bicycle

Finally, a special thank goes to my supervisor Mykhaylo Semtsiv, who, with inexhaustible patience and support, made this thesis possible.

Selbständigkeitserklärung

Ich erkläre hiermit, dass ich die vorliegende Arbeit selbstständig verfasst und noch nicht für andere Prüfungen eingereicht habe. Sämtliche Quellen einschlieÃlich Internetquellen, die unverändert oder abgewandelt wiedergegeben werden, insbesondere Quellen für Texte, Grafiken, Tabellen und Bilder, sind als solche kenntlich gemacht. Mir ist bekannt, dass bei VerstöÃen gegen diese Grundsätze ein Verfahren wegen Täuschungsversuchs bzw. Täuschung eingeleitet wird.

Berlin, den _____

_____

Irene La Penna